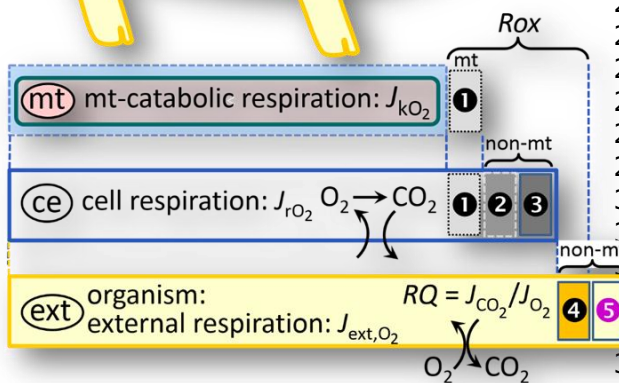
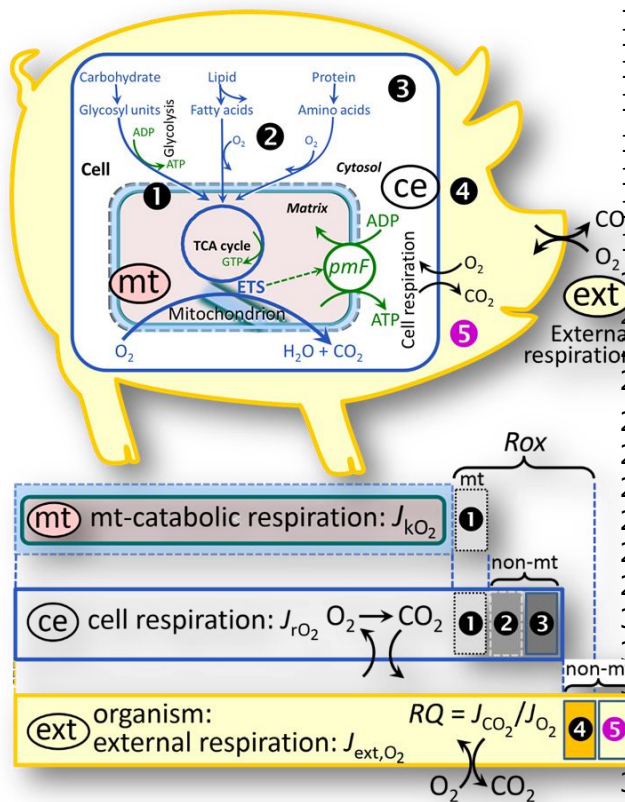


# Mitochondrial physiology

## 2. Respiratory states and rates

MitoEAGLE Task Group\*

*Living Communication:* extended resource of **Mitochondrial respiratory states and rates. Nat Metab** (Gnaiger *et al*, in review); from Gnaiger *et al* (2020) Bioenerg Commun 2020.1.



### Overview

#### Internal and external respiration

(mt) **Mitochondrial catabolic respiration**,  $J_{kO_2}$ , is the  $O_2$  consumption in the oxidation of fuel substrates (electron donors) and reduction of  $O_2$  catalysed by the electron transfer system, ETS, which drives the protonmotive force,  $pmF$ .  $J_{kO_2}$  excludes mitochondrial residual oxygen consumption, mt-Rox (1).

(ce) **Cell respiration** or internal cellular  $O_2$  consumption,  $J_{rO_2}$ , takes into account all chemical reactions,  $r$ , that consume  $O_2$  in the cells. Catabolic cell respiration is the  $O_2$  consumption associated with catabolic pathways in the cell, including (mt) mitochondrial catabolism; mt-Rox (1); non-mt  $O_2$  consumption by catabolic reactions, particularly peroxisomal oxidases and microsomal cytochrome P450 systems (2); and non-mt  $Rox$  by reactions unrelated to catabolism (3).

(ext) **External respiration** balances internal respiration at steady-state,

including extracellular  $Rox$  (4) and aerobic respiration by the microbiome (5).

$O_2$  is transported from the environment across the respiratory cascade, *i.e.*, circulation between tissues and diffusion across cell membranes, to the intracellular compartment. The respiratory quotient,  $RQ$ , is the molar  $CO_2/O_2$  exchange ratio; when combined with the respiratory nitrogen quotient,  $N/O_2$  (mol N given off per mol  $O_2$  consumed), the  $RQ$  reflects the proportion of carbohydrate, lipid and protein utilized in cell respiration during aerobically balanced steady-states. Bicarbonate and  $CO_2$  are transported in reverse to the extracellular milieu and the organismic environment. Hemoglobin provides the molecular paradigm for the combination of  $O_2$  and  $CO_2$  exchange, as do lungs, gills, the skin and other surfaces on the morphological level.

Respiratory states are defined in **Table 1**. Rates are illustrated in **Figure 5**. Consult **Table 8** for a list of terms and symbols.

### Updates:

[https://www.bioenergetics-communications.org/index.php/BEC2020.1\\_doi10.26124bec2020-0001.v1](https://www.bioenergetics-communications.org/index.php/BEC2020.1_doi10.26124bec2020-0001.v1)

Table and Figure numbers refer to Gnaiger *et al* (2020) Bioenerg Commun 2020.1.

### Table of contents

56	Abstract – Executive summary
57	1. States and rates
58	2. Coupling states and rates in mitochondrial preparations
59	2.1. Cellular and mitochondrial respiration
60	2.1.1. Aerobic and anaerobic catabolism and ATP turnover
61	2.1.2. Specification of biochemical dose
62	2.2. Mitochondrial preparations
63	2.3. Electron transfer pathways
64	2.4. Respiratory coupling control
65	2.4.1. Coupling
66	2.4.2. Phosphorylation, $P_{\gg}$ , and $P_{\gg}/O_2$ ratio
67	2.4.3. Uncoupling
68	2.5. Coupling states and respiratory rates
69	2.5.1. LEAK-state
70	2.5.2. OXPHOS-state
71	2.5.3. Electron transfer-state
72	2.5.4. ROX state and $R_{ox}$
73	2.5.5. Quantitative relations
74	2.5.6. The steady-state
75	2.6. Classical terminology for isolated mitochondria
76	2.6.1. – 2.6.5. State 1 – State 5
77	2.7. Control and regulation
78	3. What is a rate? – Box 1: Metabolic flows and fluxes: vectorial, vectorial, and scalar
79	4. Normalization of rate per sample
80	4.1. Flow: per object
81	4.1.1. Number concentration
82	4.1.2. Flow per object
83	4.2. Size-specific flux: per sample size
84	4.2.1. Sample concentration
85	4.2.2. Size-specific flux
86	4.3. Marker-specific flux: per mitochondrial content
87	5. Normalization of rate per system
88	5.1. Flow: per chamber
89	5.2. Flux: per chamber volume
90	5.2.1. System-specific flux
91	5.2.2. Advancement per volume
92	6. Conversion of units
93	7. Conclusions – Box 2: Recommendations for studies with mitochondrial preparations
94	References
95	Authors (MitoEAGLE Task Group) – Author contributions
96	Acknowledgements – Competing financial interests – Correspondence
97	

## Abstract

As the knowledge base and importance of mitochondrial physiology to evolution, health and disease expands, the necessity for harmonizing the terminology concerning mitochondrial respiratory states and rates has become increasingly apparent. The chemiosmotic theory establishes the mechanism of energy transformation and coupling in oxidative phosphorylation. The unifying concept of the protonmotive force provides the framework for developing a consistent theoretical foundation of mitochondrial physiology and bioenergetics. We follow guidelines of the International Union of Pure and Applied Chemistry (IUPAC) on terminology in physical chemistry, extended by considerations of open systems and thermodynamics of irreversible processes. The concept-driven constructive terminology incorporates the meaning of each quantity and aligns concepts and symbols with the nomenclature of classical bioenergetics. We endeavour to provide a balanced view of mitochondrial respiratory control and a critical discussion on reporting

112 **data of mitochondrial respiration in terms of metabolic flows and fluxes. Uniform**  
113 **standards for evaluation of respiratory states and rates will ultimately contribute to**  
114 **reproducibility between laboratories and thus support the development of databases of**  
115 **mitochondrial respiratory function in species, tissues, and cells. Clarity of concept and**  
116 **consistency of nomenclature facilitate effective transdisciplinary communication,**  
117 **education, and ultimately further discovery.**  
118

119 *Keywords:* Mitochondrial respiratory control, coupling control, mitochondrial preparations,  
120 protonmotive force, uncoupling, oxidative phosphorylation: OXPHOS, efficiency, electron  
121 transfer: ET, electron transfer system: ETS, proton leak, ion leak and slip compensatory state:  
122 LEAK, residual oxygen consumption: ROX, State 2, State 3, State 4, normalization, flow, flux,  
123 oxygen: O<sub>2</sub>  
124

## 125 **Executive summary**

126  
127 In view of the broad implications for health care, mitochondrial researchers face an increasing  
128 responsibility to disseminate their fundamental knowledge and novel discoveries to a wide range  
129 of stakeholders and scientists beyond the group of specialists. This requires implementation of a  
130 commonly accepted terminology within the discipline and standardization in the translational  
131 context. Authors, reviewers, journal editors, and lecturers are challenged to collaborate with the  
132 aim to harmonize the nomenclature in the growing field of mitochondrial physiology and  
133 bioenergetics, from evolutionary biology and comparative physiology to mitochondrial medicine.  
134 In the present communication we focus on the following concepts in mitochondrial physiology:  
135

136 1. Aerobic respiration is the O<sub>2</sub> flux in catabolic reactions coupled to phosphorylation of ADP to  
137 ATP, and O<sub>2</sub> flux in a variety of O<sub>2</sub> consuming reactions apart from oxidative phosphorylation  
138 (OXPHOS). Coupling in OXPHOS is mediated by the translocation of protons across the  
139 mitochondrial inner membrane (mtIM) through proton pumps generating or utilizing the  
140 protonmotive force that is maintained between the mitochondrial matrix and intermembrane  
141 compartment or outer mitochondrial space. Compartmental coupling depends on ion  
142 translocation across a semipermeable membrane, which is defined as vectorial metabolism and  
143 distinguishes OXPHOS from cytosolic fermentation as counterparts of cellular core energy  
144 metabolism (**Overview**). Cell respiration is thus distinguished from fermentation: (1) Electron  
145 acceptors are supplied by external respiration for the maintenance of redox balance, whereas  
146 fermentation is characterized by an internal electron acceptor produced in intermediary  
147 metabolism. In aerobic cell respiration, redox balance is maintained by O<sub>2</sub> as the electron acceptor.  
148 (2) Compartmental coupling in vectorial OXPHOS contrasts to exclusively scalar substrate-level  
149 phosphorylation in fermentation.  
150

151 2. When measuring mitochondrial metabolism, the contribution of fermentation and other  
152 cytosolic interactions must be excluded from analysis by disrupting the barrier function of the  
153 plasma membrane. Selective removal or permeabilization of the plasma membrane yields  
154 mitochondrial preparations—including isolated mitochondria, tissue and cellular preparations—  
155 with structural and functional integrity. Subsequently, extramitochondrial concentrations of fuel  
156 substrates, ADP, ATP, inorganic phosphate, and cations including H<sup>+</sup> can be controlled to  
157 determine mitochondrial function under a set of conditions defined as coupling control states. We  
158 strive to incorporate an easily recognized and understood concept-driven terminology of  
159 bioenergetics with explicit terms and symbols that define the nature of respiratory states.  
160

161 3. Mitochondrial coupling states are defined according to the control of respiratory oxygen flux  
162 by the protonmotive force, *pmF*, in an interaction of the electron transfer system generating the  
163 *pmF* and the phosphorylation system utilizing the *pmF*. Capacities of OXPHOS and electron  
164 transfer are measured at kinetically-saturating concentrations of fuel substrates, ADP and  
165 inorganic phosphate, and O<sub>2</sub>, or at optimal uncoupler concentrations, respectively, in the absence  
166 of Complex IV inhibitors such as NO, CO, or H<sub>2</sub>S. Respiratory capacity is a measure of the upper  
167 boundary of the rate of respiration; it depends on the substrate type undergoing oxidation in a  
168 mitochondrial pathway, and provides reference values for the diagnosis of health and disease.

169 Evaluation of the impact of evolutionary background, age, gender and sex, lifestyle and  
170 environment represents a major challenge for mitochondrial respiratory physiology and  
171 pathology.

172  
173 4. Incomplete tightness of coupling, *i.e.*, some degree of uncoupling relative to the mitochondrial  
174 pathway-dependent coupling stoichiometry, is a characteristic of energy-transformations across  
175 membranes. Uncoupling is caused by a variety of physiological, pathological, toxicological,  
176 pharmacological and environmental conditions that exert an influence not only on the proton leak  
177 and cation cycling, but also on proton slip within the proton pumps and the structural integrity of  
178 the mitochondria. A more loosely coupled state is induced by stimulation of mitochondrial  
179 superoxide formation and the bypass of proton pumps. In addition, the use of protonophores  
180 represents an experimental uncoupling intervention to assess the transition from a well-coupled  
181 to a noncoupled state of mitochondrial respiration.

182  
183 5. Respiratory oxygen consumption rates have to be carefully normalized to enable meta-analytic  
184 studies beyond the question of a particular experiment. Therefore, all raw data on rates and  
185 variables for normalization should be published in an open access data repository. Normalization  
186 of rates for: (1) the number of objects (cells, organisms); (2) the volume or mass of the  
187 experimental sample; and (3) the concentration of mitochondrial markers in the instrumental  
188 chamber are sample-specific normalizations, which are distinguished from system-specific  
189 normalization for the volume of the instrumental chamber (the measuring system).

190  
191 6. The consistent use of terms and symbols facilitates transdisciplinary communication and will  
192 support the further development of a collaborative database on bioenergetics and mitochondrial  
193 physiology.

194

## 195 **1. States and rates**

196

197 Mitochondria are the powerhouses of the cell with numerous morphological, physiological,  
198 molecular, and genetic functions. Every study of mitochondrial health and disease faces Evolution,  
199 Age, Gender and sex, Lifestyle, and Environment (MitoEAGLE) as essential background conditions  
200 intrinsic to the individual person or cohort, species, tissue and to some extent even cell line. As a  
201 large and coordinated group of laboratories and researchers, the mission of the global MitoEAGLE  
202 Network is to generate the necessary scale, type, and quality of consistent data sets and conditions  
203 to address this intrinsic complexity. Harmonization of experimental protocols and  
204 implementation of a quality control and data management system are required to interrelate  
205 results gathered across a spectrum of studies and to generate a rigorously monitored database  
206 focused on mitochondrial respiratory function. In this way, researchers from a variety of  
207 disciplines can compare their findings using clearly defined and accepted international standards.

208 With an emphasis on quality of research, published data can be useful far beyond the specific  
209 question of a particular experiment. For example, collaborative data sets support the development  
210 of open-access databases such as those for National Institutes of Health sponsored research in  
211 genetics, proteomics, and metabolomics. Indeed, enabling meta-analysis is the most economic  
212 way of providing robust answers to biological questions (Cooper *et al* 2009). However, the  
213 reproducibility of quantitative results depend on accurate measurements under strictly-defined  
214 conditions. Likewise, meaningful interpretation and comparability of experimental outcomes  
215 requires harmonization of protocols between research groups at different institutes. In addition  
216 to quality control, a conceptual framework is also required to standardise and harmonise  
217 terminology and methodology. Vague or ambiguous jargon can lead to confusion and may convert  
218 valuable signals to wasteful noise. For this reason, measured values must be expressed in standard  
219 units for each parameter used to define mitochondrial respiratory function. A consensus on  
220 fundamental nomenclature and conceptual coherence, however, are missing in the expanding  
221 field of mitochondrial physiology. To fill this gap, the present communication provides an in-depth  
222 review on harmonization of nomenclature and definition of technical terms, which are essential  
223 to improve the awareness of the intricate meaning of current and past scientific vocabulary. This



224 is important for documentation and integration into data repositories in general, and quantitative  
225 modelling in particular (Beard 2005).

226 In this review, we focus on coupling states and fluxes through metabolic pathways of aerobic  
227 energy transformation in mitochondrial preparations in the attempt to establish a conceptually-  
228 oriented nomenclature in bioenergetics and mitochondrial physiology in a series of  
229 communications, prepared in the frame of the EU COST Action MitoEAGLE open to global bottom-  
230 up input. [Reference to Part 1. Quantitative mitochondrial physiology. Mitochondria and bioblasts](#)

231

## 232 **2. Coupling states and rates in mitochondrial preparations**

233

234 *'Every professional group develops its own technical jargon for talking about matters of critical*  
235 *concern ... People who know a word can share that idea with other members of their group, and*  
236 *a shared vocabulary is part of the glue that holds people together and allows them to create a*  
237 *shared culture'* (Miller 1991).

238

### 239 *2.1. Cellular and mitochondrial respiration*

240

241 **2.1.1. Aerobic and anaerobic catabolism and ATP turnover:** In respiration, electron transfer  
242 is coupled to the phosphorylation of ADP to ATP, with energy transformation mediated by the  
243 protonmotive force,  $pmF$  (**Figure 2**). Anabolic reactions are coupled to catabolism, both by ATP  
244 as the intermediary energy currency and by small organic precursor molecules as building blocks  
245 for biosynthesis (Diebold *et al* 2019). Glycolysis involves substrate-level phosphorylation of ADP  
246 to ATP in fermentation without utilization of  $O_2$ , studied mainly in living cells and organisms. Many  
247 cellular fuel substrates are catabolized to acetyl-CoA or to glutamate, and further electron transfer  
248 reduces nicotinamide adenine dinucleotide to NADH or flavin adenine dinucleotide to  $FADH_2$ .  
249 Subsequent mitochondrial electron transfer to  $O_2$  is coupled to proton translocation for the  
250 control of the protonmotive force and phosphorylation of ADP (**Figure 1b and 1c**). In  
251 contrast, extramitochondrial oxidation of fatty acids and amino acids proceeds partially in  
252 peroxisomes without coupling to ATP production: acyl-CoA oxidase catalyzes the oxidation of  
253  $FADH_2$  with electron transfer to  $O_2$ ; amino acid oxidases oxidize flavin mononucleotide  $FMN$  or  
254  $FADH_2$  (**Figure 1a**).

255 The plasma membrane separates the intracellular compartment including the cytosol, nucleus,  
256 and organelles from the extracellular environment. Cell membranes include the plasma  
257 membrane and organellar membranes. The plasma membrane consists of a lipid bilayer with  
258 embedded proteins and attached organic molecules that collectively control the selective  
259 permeability of ions, organic molecules, and particles across the cell boundary. The intact plasma  
260 membrane prevents the passage of many water-soluble mitochondrial substrates and inorganic  
261 ions—such as succinate, adenosine diphosphate (ADP) and inorganic phosphate ( $P_i$ ) that must be  
262 precisely controlled at kinetically-saturating concentrations for the analysis of mitochondrial  
263 respiratory capacities (**Figure 2**). Respiratory capacities delineate, comparable to channel  
264 capacity in information theory (Schneider 2006), the upper boundary of the rate of  $O_2$   
265 consumption measured in defined respiratory states. The intact plasma membrane limits the  
266 scope of investigations into mitochondrial respiratory function in living cells, despite the activity  
267 of solute carriers, *e.g.*, the sodium-dependent dicarboxylate transporter SLC13A3 and the sodium-  
268 dependent phosphate transporter SLC20A2, which transport specific metabolites across the  
269 plasma membrane of various cell types, and the availability of plasma membrane-permeable  
270 succinate (Ehinger *et al* 2016). These limitations are overcome by the use of mitochondrial  
271 preparations.

272

273 **2.1.2. Specification of biochemical dose:** Substrates, uncouplers, inhibitors, and other chemical  
274 reagents are titrated to analyse cellular and mitochondrial function. Nominal concentrations of  
275 these substances are usually reported as initial amount of substance concentration [ $mol \cdot L^{-1}$ ] in the  
276 incubation medium.

277 Kinetically-saturating conditions are evaluated by substrate kinetics to obtain the maximum  
278 reaction velocity or maximum pathway flux, in contrast to solubility-saturated conditions. When  
279 aiming at the measurement of kinetically-saturated processes—such as OXPPOS-capacities—the  
280 concentrations for substrates can be chosen according to half-saturating substrate  
281 concentrations,  $c_{50}$ , for metabolic pathways, or the Michaelis constant,  $K_m$ , for enzyme kinetics. In  
282 the case of hyperbolic kinetics, only 80 % of maximum respiratory capacity is obtained at a  
283 substrate concentration of four times the  $c_{50}$ , whereas substrate concentrations of 5, 9, 19 and 49  
284 times the  $c_{50}$  are theoretically required for reaching 83 %, 90 %, 95 % or 98 % of the maximal rate  
285 (Gnaiger 2001).

286 Other reagents are chosen to inhibit or alter a particular process. The amount of these  
287 chemicals in an experimental incubation is selected to maximize effect, avoiding unacceptable off-  
288 target consequences that would adversely affect the data being sought. Specifying the amount of  
289 substance in an incubation as nominal concentration in the aqueous incubation medium can be  
290 ambiguous (Doskey *et al* 2015), particularly for cations (TPP<sup>+</sup>; fluorescent dyes such as safranin,  
291 TMRM; Chowdhury *et al* 2015) and lipophilic substances (oligomycin, uncouplers,  
292 permeabilization agents; Doerrier *et al* 2018), which accumulate in the mitochondrial matrix or  
293 in biological membranes, respectively. Generally, dose/exposure can be specified per unit of  
294 biological sample, *i.e.*, (nominal moles of xenobiotic)/(number of cells) [ $\text{mol}\cdot\text{cell}^{-1}$ ] or, as  
295 appropriate, per mass of biological sample [ $\text{mol}\cdot\text{kg}^{-1}$ ]. This approach to specification of  
296 dose/exposure provides a scalable parameter that can be used to design experiments, help  
297 interpret a wide variety of experimental results, and provide absolute information that allows  
298 researchers worldwide to make the most use of published data (Doskey *et al* 2015).

299

## 300 2.2. Mitochondrial preparations

301

302 Mitochondrial preparations are defined as either isolated mitochondria or tissue and cellular  
303 preparations in which the barrier function of the plasma membrane is disrupted. Since this entails  
304 the loss of cell viability, mitochondrial preparations are not studied *in vivo*. In contrast to isolated  
305 mitochondria and tissue homogenate preparations, mitochondria in permeabilized tissues and  
306 cells are *in situ* relative to the plasma membrane. When studying mitochondrial preparations,  
307 substrate-uncoupler-inhibitor-titration (SUIT) protocols are used to establish respiratory  
308 coupling control states (CCS) and pathway control states (PCS) that provide reference values for  
309 various output variables (**Table 1**). Physiological conditions *in vivo* deviate from these  
310 experimentally obtained states; this is because kinetically-saturating concentrations, *e.g.*, of ADP,  
311 oxygen ( $\text{O}_2$ ; dioxygen) or fuel substrates, may not apply to physiological intracellular conditions.  
312 Further information is obtained in studies of kinetic responses to variations in fuel substrate  
313 concentrations, [ADP], or [ $\text{O}_2$ ] in the range between kinetically-saturating concentrations and  
314 anoxia (Gnaiger 2001).

315 The cholesterol content of the plasma membrane is high compared to mitochondrial  
316 membranes (Korn 1969). Therefore, mild detergents—such as digitonin and saponin—can be  
317 applied to selectively permeabilize the plasma membrane via interaction with cholesterol; this  
318 allows free exchange of organic molecules and inorganic ions between the cytosol and the  
319 immediate cell environment, while maintaining the integrity and localization of organelles,  
320 cytoskeleton, and the nucleus. Application of permeabilization agents (mild detergents or toxins)  
321 leads to washout of cytosolic marker enzymes—such as lactate dehydrogenase—and results in  
322 the complete loss of cell viability (tested by nuclear staining using plasma membrane-  
323 impermeable dyes), while mitochondrial function remains intact (tested by cytochrome *c*  
324 stimulation of respiration). Digitonin concentrations have to be optimized according to cell  
325 type, particularly since mitochondria from cancer cells contain significantly higher contents of  
326 cholesterol in both membranes (Baggetto and Testa-Perussini, 1990). For example, a dose of  
327 digitonin of  $8 \text{ fmol}\cdot\text{cell}^{-1}$  ( $10 \text{ pg}\cdot\text{cell}^{-1}$ ;  $10 \mu\text{g}\cdot 10^{-6} \text{ cells}$ ) is optimal for permeabilization of  
328 endothelial cells, and the concentration in the incubation medium has to be adjusted according to  
329 the cell concentration (Doerrier *et al* 2018). Respiration of isolated mitochondria remains  
330 unaltered after the addition of low concentrations of digitonin or saponin. In addition to

331 mechanical cell disruption during homogenization of tissue, permeabilization agents may be  
332 applied to ensure permeabilization of all cells in tissue homogenates.

333 Suspensions of cells permeabilized in the respiration chamber and crude tissue homogenates  
334 contain all components of the cell at highly dilute concentrations. All mitochondria are retained  
335 in chemically-permeabilized mitochondrial preparations and crude tissue homogenates. In the  
336 preparation of isolated mitochondria, however, the mitochondria are separated from other cell  
337 fractions and purified by differential centrifugation, entailing the loss of mitochondria at typical  
338 recoveries ranging from 30 % to 80 % of total mitochondrial content (Lai *et al* 2018). Using Percoll  
339 or sucrose density gradients to maximize the purity of isolated mitochondria may compromise  
340 the mitochondrial yield or structural and functional integrity. Therefore, mitochondrial isolation  
341 protocols need to be optimized according to each study. The term *mitochondrial preparation*  
342 neither includes living cells, nor submitochondrial particles and further fractionated  
343 mitochondrial components.

344

### 345 2.3. Electron transfer pathways

346

347 Mitochondrial electron transfer (ET) pathways are fuelled by diffusion and transport of substrates  
348 across the mtOM and mtIM. In addition, the mitochondrial electron transfer system (ETS) consists  
349 of the matrix-ETS and membrane-ETS (**Figure 1b**). Upstream sections of ET-pathways converge  
350 at the NADH-junction (N-junction). NADH is mainly generated in the tricarboxylic acid (TCA) cycle  
351 and is oxidized by Complex I (CI), with further electron entry into the coenzyme Q-junction (Q-  
352 junction). Similarly, succinate is formed in the TCA cycle and oxidized by CII to fumarate. CII is  
353 part of both the TCA cycle and the ETS, and reduces FAD to FADH<sub>2</sub> with further reduction of  
354 ubiquinone to ubiquinol downstream of the TCA cycle in the Q-junction. Thus FADH<sub>2</sub> is not a  
355 substrate but is the product of CII, in contrast to erroneous metabolic maps shown in many  
356 publications.  $\beta$ -oxidation of fatty acids (FA) supplies reducing equivalents via (1) FADH<sub>2</sub> as the  
357 substrate of electron transferring flavoprotein complex (ETF); (2) acetyl-CoA generated by chain  
358 shortening; and (3) NADH generated via 3-hydroxyacyl-CoA dehydrogenases. The ATP yield  
359 depends on whether acetyl-CoA enters the TCA cycle, or is for example used in ketogenesis.

360 Selected mitochondrial catabolic pathways of electron transfer from the oxidation of fuel  
361 substrates to the reduction of O<sub>2</sub> are stimulated by addition of fuel substrates to the mitochondrial  
362 respiration medium after depletion of endogenous substrates (**Figure 1b**). Substrate  
363 combinations and specific inhibitors of ET-pathway enzymes are used to obtain defined pathway  
364 control states in mitochondrial preparations (Gnaiger 2020).

365

### 366 2.4. Respiratory coupling control

367

368 **2.4.1. Coupling:** In mitochondrial electron transfer, vectorial transmembrane proton flux is  
369 coupled through the redox proton pumps CI, CIII and CIV to the catabolic flux of scalar reactions,  
370 collectively measured as O<sub>2</sub> flux,  $J_{\text{ko}_2}$  (**Figure 1**). Thus mitochondria are elementary components  
371 of energy transformation. Energy is a conserved quantity and cannot be lost or produced in any  
372 internal process (First Law of Thermodynamics). Open and closed systems can gain or lose energy  
373 only by external fluxes—by exchange with the environment. Therefore, energy can neither be  
374 produced by mitochondria, nor is there any internal process without energy conservation. Exergy  
375 or Gibbs energy ('free energy') is the part of energy that can potentially be transformed into work  
376 under conditions of constant temperature and pressure. *Coupling* is the interaction of an  
377 exergonic process (spontaneous, negative exergy change) with an endergonic process (positive  
378 exergy change) in energy transformations which conserve part of the exergy change. Exergy is not  
379 completely conserved, however, except at the limit of 100 % efficiency of energy transformation  
380 in a coupled process. The exergy or Gibbs energy change that is not conserved by coupling is  
381 irreversibly lost or dissipated, and is accounted for as the entropy change of the surroundings and  
382 the system, multiplied by the temperature of the irreversible process.

383 Pathway control states (PCS) and coupling control states (CCS) are complementary, since  
 384 mitochondrial preparations depend on (1) an exogenous supply of pathway-specific fuel  
 385 substrates and oxygen, and (2) exogenous control of phosphorylation (Figure 1).  
 386

387 **2.4.2. Phosphorylation, P<sub>»</sub>, and P<sub>»</sub>/O<sub>2</sub> ratio:** Phosphorylation in the context of OXPHOS is  
 388 defined as phosphorylation of ADP by P<sub>i</sub> to form ATP. On the other hand, the term phosphorylation  
 389 is used generally in many contexts, e.g., protein phosphorylation. This provides the argument for  
 390 introducing a symbol more discriminating and specific than P as used in the P/O ratio (phosphate  
 391 to atomic oxygen ratio), where P indicates phosphorylation of ADP to ATP or GDP to GTP (Figure  
 392 1): The symbol P<sub>»</sub> indicates the endergonic (uphill) direction of phosphorylation ADP→ATP, and  
 393 likewise P<sub>«</sub> the corresponding exergonic (downhill) hydrolysis ATP→ADP. P<sub>»</sub> refers mainly to  
 394 electrontransfer phosphorylation but may also involve substrate-level phosphorylation as part of  
 395 the TCA cycle (succinyl-CoA ligase, phosphoglycerate kinase) and phosphorylation of ADP  
 396 catalyzed by pyruvate kinase, and of GDP phosphorylated by phosphoenolpyruvate  
 397 carboxykinase. Transphosphorylation is performed by adenylate kinase, creatine kinase (mtCK),  
 398 hexokinase and nucleoside diphosphate kinase. In isolated mammalian mitochondria, ATP  
 399 production catalyzed by adenylate kinase (2 ADP ↔ ATP + AMP) proceeds without fuel substrates  
 400 in the presence of ADP (Kömödi and Tretter 2017). Kinase cycles are involved in intracellular  
 401 energy transfer and signal transduction for regulation of energy flux. The P<sub>»</sub>/O<sub>2</sub> ratio (P<sub>»</sub>/4 e<sup>-</sup>) is  
 402 two times the 'P/O' ratio (P<sub>»</sub>/2 e<sup>-</sup>). P<sub>»</sub>/O<sub>2</sub> is a generalized symbol, not specific for reporting P<sub>i</sub>  
 403 consumption (P<sub>i</sub>/O<sub>2</sub> flux ratio), ADP depletion (ADP/O<sub>2</sub> flux ratio), or ATP production (ATP/O<sub>2</sub>  
 404 flux ratio). The mechanistic P<sub>»</sub>/O<sub>2</sub> ratio—or P<sub>»</sub>/O<sub>2</sub> stoichiometry—is calculated from the proton-  
 405 to-O<sub>2</sub> and proton-to-phosphorylation coupling stoichiometries (Figure 1c):

$$407 \quad P_{\gg}/O_2 = \frac{H_{\text{pos}}^+/O_2}{H_{\text{neg}}^+/P_{\gg}} \quad (1)$$

408  
 409 The H<sup>+</sup><sub>pos</sub>/O<sub>2</sub> coupling stoichiometry (referring to the full four electron reduction of O<sub>2</sub>) depends  
 410 on the relative involvement of the three coupling sites (respiratory Complexes CI, CIII and CIV) in  
 411 the catabolic ET-pathway from reduced fuel substrates (electron donors) to the reduction of O<sub>2</sub>  
 412 (electron acceptor). This varies with: (1) a bypass of CI by single or multiple electron input into  
 413 the Q-junction; and (2) a bypass of CIV by involvement of alternative oxidases, AOX. AOX are  
 414 expressed in all plants, some fungi, many protists, and several animal phyla, but are not expressed  
 415 in vertebrate mitochondria (McDonald *et al* 2009).  
 416

417 The H<sup>+</sup><sub>pos</sub>/O<sub>2</sub> coupling stoichiometry equals 12 in the ET-pathways involving CIII and CIV as  
 418 proton pumps, increasing to 20 for the NADH-pathway through CI (Figure 1b). A general  
 419 consensus on H<sup>+</sup><sub>pos</sub>/O<sub>2</sub> stoichiometries, however, remains to be reached (Hinkle 2005; Wikström  
 420 and Hummer 2012; Sazanov 2015). The H<sup>+</sup><sub>neg</sub>/P<sub>»</sub> coupling stoichiometry (3.7; Figure 1b) is the  
 421 sum of 2.7 H<sup>+</sup><sub>neg</sub> required by the F<sub>1</sub>F<sub>0</sub>-ATPase of vertebrate and most invertebrate species (Watt  
 422 *et al* 2010) and the proton balance in the translocation of ADP, ATP and P<sub>i</sub> (Figure 1c). Taken  
 423 together, the mechanistic P<sub>»</sub>/O<sub>2</sub> ratio is calculated at 5.4 and 3.3 for the N- and S-pathway,  
 424 respectively (Eq. 1). The corresponding classical P<sub>»</sub>/O ratios (referring to the 2 electron reduction  
 425 of 0.5 O<sub>2</sub>) are 2.7 and 1.6 (Watt *et al* 2010), in agreement with the measured P<sub>»</sub>/O ratio for  
 426 succinate of 1.58 ± 0.02 (Gnaiger *et al* 2000).  
 427

428 **2.4.3. Uncoupling:** The effective P<sub>»</sub>/O<sub>2</sub> flux ratio (Y<sub>P<sub>»</sub>/O<sub>2</sub></sub> = J<sub>P<sub>»</sub></sub>/J<sub>kO<sub>2</sub></sub>) is diminished relative to the  
 429 mechanistic P<sub>»</sub>/O<sub>2</sub> ratio by intrinsic and extrinsic uncoupling or dyscoupling (Figure 3). This is  
 430 distinct from switching between mitochondrial pathways that involve fewer than three proton  
 431 pumps ('coupling sites': Complexes CI, CIII and CIV), bypassing CI through multiple electron  
 432 entries into the Q-junction, or bypassing CIII and CIV through AOX (Figure 1b). Reprogramming  
 433 of mitochondrial pathways leading to different types of substrates being oxidized may be  
 434 considered as a switch of gears (changing the stoichiometry by altering the substrate that is  
 435 oxidized) rather than uncoupling (loosening the tightness of coupling relative to a fixed  
 436 stoichiometry). In addition, Y<sub>P<sub>»</sub>/O<sub>2</sub></sub> depends on several experimental conditions of flux control,



437 increasing as a hyperbolic function of [ADP] to a maximum value (Gnaiger 2001). Uncoupling of  
438 mitochondrial respiration is a general term comprising diverse mechanisms (**Figure 3**):

- 439  
440 1. Proton leak across the mtIM from the positive to the negative compartment ( $H^+$  leak-  
441 uncoupled);  
442 2. Cycling of other cations, strongly stimulated by mtPT; comparable to the use of protonophores,  
443 cation cycling is experimentally induced by valinomycin in the presence of  $K^+$   
444 3. Decoupling by proton slip in the redox proton pumps (CI, CIII and CIV) when protons are  
445 effectively not pumped in the ETS, or are not driving phosphorylation ( $F_1F_0$ -ATPase)  
446 4. Loss of vesicular (compartmental) integrity when electron transfer is uncoupled  
447 5. Electron leak in the loosely coupled univalent reduction of  $O_2$  to superoxide ( $O_2^{\cdot-}$ ; superoxide  
448 anion radical)  
449

450 Differences of terms—uncoupled vs. noncoupled—are easily overlooked, although they relate  
451 to different meanings of uncoupling (**Table 2** and **Figure 3**).  
452

### 453 2.5. Coupling states and respiratory rates

454  
455 To extend the classical nomenclature on mitochondrial coupling states (Section 2.6) by a concept-  
456 driven terminology that explicitly incorporates information on the meaning of respiratory states,  
457 the terminology must be general and not restricted to any particular experimental protocol or  
458 mitochondrial preparation (Gnaiger 2009). Diagnostically meaningful and reproducible  
459 conditions are defined for measuring mitochondrial function and respiratory capacities of core  
460 energy metabolism. Standard respiratory coupling states are obtained while maintaining a  
461 defined ET-pathway state with constant fuel substrates and inhibitors of specific branches of the  
462 ET-pathway. Concept-driven nomenclature aims at mapping the meaning and concept behind the  
463 words and acronyms onto the forms of words and acronyms (Miller 1991). The focus of concept-  
464 driven nomenclature is primarily the conceptual *why*, along with clarification of the experimental  
465 *how* (**Table 1**).  
466

467 **LEAK**: The contribution of intrinsically uncoupled  $O_2$  consumption is studied by preventing the  
468 stimulation of phosphorylation either in the absence of ADP or by inhibition of the  
469 phosphorylation-pathway. The corresponding states are collectively classified as LEAK-states  
470 when  $O_2$  consumption compensates mainly for ion leaks, including the proton leak.

471 **OXPHOS**: The ET- and phosphorylation-pathways comprise coupled segments of the OXPHOS-  
472 system and provide reference values of respiratory capacities. The OXPHOS-capacity is  
473 measured at kinetically-saturating concentrations of ADP and  $P_i$ .

474 **ET**: Compared to OXPHOS-capacity, the oxidative ET-capacity reveals the limitation of OXPHOS-  
475 capacity mediated by the phosphorylation-pathway. By application of external uncouplers, ET-  
476 capacity is measured as noncoupled respiration. The three coupling states, LEAK, OXPHOS, and  
477 ET are shown schematically with the corresponding respiratory rates, abbreviated as *L*, *P*, and  
478 *E*, respectively (**Figure 2**). We distinguish between metabolic *pathways* and metabolic *states*  
479 with the corresponding metabolic *rates*; for example: ET-pathways, ET-states, and ET-  
480 capacities, *E*, respectively (**Table 1**). The protonmotive force, *pmF*, is *maximum* in the LEAK-  
481 state of coupled mitochondria, driven by LEAK-respiration at a minimum back-flux of cations  
482 to the matrix side, *high* in the OXPHOS-state when it drives phosphorylation, and *very low* in  
483 the ET-state when uncouplers short-circuit the proton cycle (**Table 1**).  
484

485 **2.5.1. LEAK-state (Figure 4a)**: The LEAK-state is defined as a state of mitochondrial respiration  
486 when  $O_2$  flux mainly compensates for ion leaks in the absence of ATP synthesis, at kinetically-  
487 saturating concentrations of  $O_2$ , respiratory fuel substrates and  $P_i$ . LEAK-respiration is measured  
488 to obtain an estimate of intrinsic uncoupling without addition of an experimental uncoupler: (1)  
489 in the absence of adenylates, *i.e.*, AMP, ADP and ATP; (2) after depletion of ADP at a maximum  
490 ATP/ADP ratio; or (3) after inhibition of the phosphorylation-pathway by inhibitors of  $F_1F_0$ -  
491 ATPase (oligomycin), or adenine nucleotide translocase (carboxyatractyloside). Adjustment of

492 the nominal concentration of these inhibitors to the concentration of biological sample applied  
493 can minimize or avoid inhibitory side-effects exerted on ET-capacity or even some dyscoupling.  
494 The chelator EGTA is added to mt-respiration media to bind free  $\text{Ca}^{2+}$ , thus limiting cation cycling.  
495 The LEAK-rate is a function of respiratory state, hence it depends on the (1) barrier function of  
496 the mtIM ('leakiness'), (2) electrochemical potential differences and concentration differences  
497 across the mtIM, and (3)  $\text{H}^+/\text{O}_2$  ratio of the ET-pathway (**Figure 1b**).

- 498 • **Proton leak and uncoupled respiration:** The intrinsic proton leak is the *uncoupled* leak  
499 current of protons in which protons diffuse across the mtIM in the dissipative direction of the  
500 downhill protonmotive force without coupling to phosphorylation (**Figure 4a**). The proton  
501 leak flux depends non-linearly on the protonmotive force (Garlid *et al* 1989; Divakaruni and  
502 Brand 2011), which is a temperature-dependent property of the mtIM and may be enhanced  
503 due to possible contamination by free fatty acids. Inducible uncoupling mediated by  
504 uncoupling protein 1 (UCP1) is physiologically controlled, *e.g.*, in brown adipose tissue. UCP1  
505 is a member of the  
506 mitochondrial carrier family that is involved in the translocation of protons across the mtIM  
507 (Jezek *et al* 2018). Consequently, this short-circuit lowers the  $pmF$  and stimulates electron  
508 transfer, respiration, and heat dissipation in the absence of phosphorylation of ADP.
- 509 • **Cation cycling:** There can be other cation contributors to leak current including calcium and  
510 probably magnesium. Calcium influx is balanced by mitochondrial  $\text{Na}^+/\text{Ca}^{2+}$  or  $\text{H}^+/\text{Ca}^{2+}$   
511 exchange, which is balanced by  $\text{Na}^+/\text{H}^+$  or  $\text{K}^+/\text{H}^+$  exchanges. This is another effective  
512 uncoupling mechanism different from proton leak (**Table 2**).
- 513 • **Proton slip and decoupled respiration:** Proton slip is the *decoupled* process in which protons  
514 are only partially translocated by a redox proton pump of the ET-pathways and slip back to the  
515 original vesicular compartment. The proton leak is the dominant contributor to the overall leak  
516 current in mammalian mitochondria incubated under physiological conditions at 37 °C,  
517 whereas proton slip increases at lower experimental temperature (Canton *et al* 1995). Proton  
518 slip can also happen in association with the  $\text{F}_1\text{F}_0$ -ATPase, in which the proton slips downhill  
519 across the pump to the matrix without contributing to ATP synthesis. In each case, proton slip  
520 is a property of the proton pump and increases with the pump turnover rate.
- 521 • **Electron leak and loosely coupled respiration:** Superoxide production by the ETS leads to a  
522 bypass of redox proton pumps and correspondingly lower  $\text{P}\gg/\text{O}_2$  ratio. This depends on the  
523 actual site of electron leak and the scavenging of hydrogen peroxide by cytochrome *c*, whereby  
524 electrons may re-enter the ETS with proton translocation by CIV.
- 525 • **Dyscoupled respiration:** Mitochondrial injuries may lead to *dyscoupling* as a pathological or  
526 toxicological cause of *uncoupled* respiration. Dyscoupling may involve any type of uncoupling  
527 mechanism, *e.g.*, opening the mtPT pore. Dyscoupled respiration is distinguished from  
528 experimentally induced *noncoupled* respiration in the ET-state (**Table 2**).
- 529 • **Protonophore titration and noncoupled respiration:** Protonophores are uncouplers which  
530 are titrated to obtain maximum *noncoupled* respiration as a measure of ET-capacity.
- 531 • **Loss of compartmental integrity and acoupled respiration:** Electron transfer and catabolic  
532  $\text{O}_2$  flux proceed without compartmental proton translocation in disrupted mitochondrial  
533 fragments. Such fragments are an artefact of mitochondrial isolation, and may not fully fuse to  
534 re-establish structurally intact mitochondria. Loss of mtIM integrity, therefore, is the cause of  
535 acoupled respiration, which is a nonvectorial dissipative process without control by the  
536 protonmotive force.

537  
538 **2.5.2. OXPHOS-state (Figure 4b):** The OXPHOS-state is defined as the respiratory state with  
539 kinetically-saturating concentrations of  $\text{O}_2$ , respiratory and phosphorylation substrates, and  
540 absence of exogenous uncoupler, which provides an estimate of the maximal respiratory capacity  
541 in the OXPHOS-state for any given ET-pathway state. Respiratory capacities at kinetically-  
542 saturating substrate concentrations provide reference values or upper limits of performance,  
543 aiming at the generation of data sets for comparative purposes. Physiological activities and effects  
544 of substrate kinetics can be evaluated relative to the OXPHOS-capacity.

545 As discussed previously, 0.2 mM ADP does not kinetically-saturate flux in isolated  
546 mitochondria (Gnaiger 2001; Puchowicz *et al* 2004); greater [ADP] is required, particularly in  
547 permeabilized muscle fibers and cardiomyocytes, to overcome limitations by intracellular  
548 diffusion and by the reduced conductance of the mtOM (Jepihhina *et al* 2011; Illaste *et al* 2012;  
549 Simson *et al* 2016), either through interaction with tubulin (Rostovtseva *et al* 2008) or other  
550 intracellular structures (Birkedal *et al* 2014). In addition, kinetically-saturating ADP  
551 concentrations need to be evaluated under different experimental conditions such as temperature  
552 (Lemieux *et al* 2017) and with different animal models (Blieher and Guderley 1993). In  
553 permeabilized muscle fiber bundles of high respiratory capacity, the apparent  $K_m$  for ADP  
554 increases up to 0.5 mM (Saks *et al* 1998), consistent with experimental evidence that >90 %  
555 kinetic saturation is reached only at >5 mM ADP (Pesta and Gnaiger 2012). Similar ADP  
556 concentrations are also required for accurate determination of OXPHOS-capacity in human  
557 clinical cancer samples and permeabilized cells (Klepinin *et al* 2016; Koit *et al* 2017). 2.5 to 5 mM  
558 ADP is sufficient to obtain the actual OXPHOS-capacity in many types of permeabilized tissue and  
559 cell preparations, but experimental validation is required in each specific case.  
560

561 **2.5.3. Electron transfer-state (Figure 4c):**  $O_2$  flux determined in the ET-state yields an estimate  
562 of ET-capacity. The ET-state is defined as the *noncoupled* state with kinetically-saturating  
563 concentrations of  $O_2$ , respiratory substrate and optimum exogenous uncoupler concentration for  
564 maximum  $O_2$  flux. Uncouplers are weak lipid-soluble acids which function as protonophores.  
565 These disrupt the barrier function of the mtIM and thus short-circuit the protonmotive system,  
566 functioning like a clutch in a mechanical system. As a consequence of the nearly collapsed  
567 protonmotive force, the driving force is insufficient for phosphorylation, and  $J_{P_s} = 0$ . The most  
568 frequently used uncouplers are carbonyl cyanide *m*-chloro phenyl hydrazone (CCCP), carbonyl  
569 cyanide *p*-trifluoromethoxyphenylhydrazone (FCCP), or dinitrophenol (DNP). Stepwise titration  
570 of uncouplers stimulates respiration up to or above the level of  $O_2$  consumption rates in the  
571 OXPHOS-state; respiration is inhibited, however, above optimum uncoupler concentrations  
572 (Mitchell 2011). Data obtained with a single dose of uncoupler must be evaluated with caution,  
573 particularly when a fixed uncoupler concentration is used in studies exploring a treatment or  
574 disease that may alter the mitochondrial content or mitochondrial sensitivity to inhibition by  
575 uncouplers. There is a need for new protonophoric uncouplers that drive maximal respiration  
576 across a broad dosing range and do not inhibit respiration at high concentrations (Kenwood *et al*  
577 2013). The effect on ET-capacity of the reversed function of  $F_1F_0$ -ATPase ( $J_{P_s}$ ; **Figure 4c**) can be  
578 evaluated in the presence and absence of extramitochondrial ATP.  
579

580 **2.5.4. ROX state:** The state of residual  $O_2$  consumption, ROX, is not a coupling state, but is relevant  
581 to assess respiratory function (**Overview**). The rate of residual oxygen consumption, *Rox*, is  
582 defined as  $O_2$  consumption due to oxidative reactions measured after inhibition of ET with  
583 rotenone, malonic acid and antimycin A. Cyanide and azide inhibit not only CIV but catalase and  
584 several peroxidases involved in *Rox*, whereas AOX is not inhibited (**Figure 1b**). High  
585 concentrations of antimycin A, but not rotenone or cyanide, inhibit peroxisomal acyl-CoA oxidase  
586 and D-amino acid oxidase (Vamecq *et al* 1987). *Rox* represents a baseline used to correct  
587 respiration measured in defined coupling control states. *Rox*-corrected *L*, *P* and *E* are not only  
588 lower than total fluxes, but also change the flux control ratios *L/P* and *L/E*. *Rox* is not necessarily  
589 equivalent to non-mitochondrial reduction of  $O_2$ , considering  $O_2$ -consuming reactions in  
590 mitochondria that are not related to ET—such as  $O_2$  consumption in reactions catalyzed by  
591 monoamine oxidases (type A and B), monooxygenases (cytochrome P450 monooxygenases),  
592 dioxygenases (trimethyllysine dioxygenase), and several hydroxylases. Isolated mitochondrial  
593 fractions, especially those obtained from liver, may be contaminated by peroxisomes, as shown  
594 by transmission electron microscopy. This fact makes the exact determination of mitochondrial  
595  $O_2$  consumption and mitochondria-associated generation of reactive oxygen species complicated  
596 (Schönfeld *et al* 2009; Speijer 2016; **Figure 1**). The variability of ROX-linked  $O_2$  consumption  
597 needs to be studied in relation to non-ET enzyme activities, availability of specific substrates,  $O_2$   
598 concentration, and electron leakage leading to the formation of reactive oxygen species.

599

600 **2.5.5. Quantitative relations:**  $E$  may exceed or be equal to  $P$ .  $E > P$  is observed in many types of  
601 mitochondria, varying between species, tissues and cell types (Gnaiger 2009).  $E - P$  is the ET-excess  
602 capacity pushing the phosphorylation-flux to the limit of its capacity for utilizing the protonmotive  
603 force (**Figure 2**). In addition, the magnitude of  $E - P$  depends on the tightness of respiratory  
604 coupling or degree of uncoupling, since an increase of  $L$  causes  $P$  to increase towards the limit of  
605  $E$  (Lemieux *et al* 2011). The ET-excess capacity,  $E - P$ , therefore, provides a sensitive diagnostic  
606 indicator of specific injuries of the phosphorylation-pathway, under conditions when  $E$  remains  
607 constant but  $P$  declines relative to controls. Substrate cocktails supporting simultaneous  
608 convergent electron transfer to the Q-junction for reconstitution of TCA cycle function establish  
609 pathway control states with high ET-capacity, and consequently increase the sensitivity of the  $E -$   
610  $P$  assay.

611  $E$  cannot theoretically be lower than  $P$ .  $E < P$  must be discounted as an artefact, which may be  
612 caused experimentally by: (1) loss of oxidative capacity during the time course of the  
613 respirometric assay, since  $E$  is measured subsequently to  $P$ ; (2) using insufficient uncoupler  
614 concentrations; (3) using high uncoupler concentrations which inhibit ET (Gnaiger 2008); (4) high  
615 oligomycin concentrations applied for measurement of  $L$  before titrations of uncoupler, when  
616 oligomycin exerts an inhibitory effect on  $E$ . On the other hand, the ET-excess capacity is  
617 overestimated if kinetically non-saturating [ADP] or [ $P_i$ ] are used. See State 3 in the next section.

618 The net OXPHOS-capacity is calculated by subtracting  $L$  from  $P$  (**Figure 2**). The net  $P \gg O_2$   
619 equals  $P \gg / (P - L)$ , wherein the dissipative LEAK component in the OXPHOS-state may be  
620 overestimated. This can be avoided by measuring LEAK-respiration in a state when the  
621 protonmotive force is adjusted to its slightly lower value in the OXPHOS-state by titration of an  
622 ET-inhibitor (Divakaruni and Brand 2011). Any turnover-dependent components of proton leak  
623 and slip, however, are underestimated under these conditions (Garlid *et al* 1993). In general, it is  
624 inappropriate to use the term *ATP production* or *ATP turnover* for the difference of  $O_2$  flux  
625 measured in the OXPHOS- and LEAK-states.  $P - L$  is the upper limit of OXPHOS-capacity that is freely  
626 available for ATP production (corrected for LEAK-respiration) and is fully coupled to  
627 phosphorylation with a maximum mechanistic stoichiometry (**Figure 2**).

628 LEAK-respiration and OXPHOS-capacity depend on (1) the tightness of coupling under the  
629 influence of the respiratory uncoupling mechanisms (**Figure 3**), and (2) the coupling  
630 stoichiometry, which varies as a function of the substrate type undergoing oxidation in ET-  
631 pathways with either two or three coupling sites (**Figure 1b**). When substrate cocktails are used  
632 supporting the convergent NADH- and succinate-pathways simultaneously, the relative  
633 contribution of ET-pathways with three or two coupling sites cannot be controlled  
634 experimentally, is difficult to determine, and may shift in transitions between LEAK-, OXPHOS-  
635 and ET-states (Gnaiger 2020). Under these experimental conditions, we cannot separate the  
636 tightness of coupling *versus* coupling stoichiometry as the mechanisms of respiratory control in a  
637 shift of  $L/P$  ratios. The tightness of coupling and fully coupled  $O_2$  flux,  $P - L$  (**Table 2**), therefore, are  
638 obtained from measurements of coupling control of LEAK-respiration, OXPHOS- and ET-  
639 capacities in well-defined pathway states, using either pyruvate and malate as substrates or the  
640 classical succinate and rotenone substrate-inhibitor combination (**Figure 1b**).

641

642 **2.5.6. The steady-state:** Mitochondria represent a thermodynamically open system in non-  
643 equilibrium states of biochemical energy transformation. State variables (protonmotive force;  
644 redox states) and metabolic *rates* (fluxes) are measured in defined mitochondrial respiratory  
645 states. Steady-states can be obtained only in open systems, in which changes by internal  
646 transformations, *e.g.*,  $O_2$  consumption, are instantaneously compensated for by external fluxes  
647 across the system boundary, *e.g.*,  $O_2$  supply, preventing a change of  $O_2$  concentration in the system  
648 (Gnaiger 1993b). Mitochondrial respiratory states monitored in closed systems satisfy the criteria  
649 of pseudo-steady states for limited periods of time, when changes in the system (concentrations  
650 of  $O_2$ , fuel substrates, ADP,  $P_i$ ,  $H^+$ ) do not exert significant effects on metabolic fluxes (respiration,  
651 phosphorylation). Such pseudo-steady states require respiratory media with sufficient buffering



652 capacity and substrates maintained at kinetically-saturating concentrations, and thus depend on  
653 the kinetics of the processes under investigation.

654  
655 **2.6. Classical terminology for isolated mitochondria**

656 *'When a code is familiar enough, it ceases appearing like a code; one forgets that there is a*  
657 *decoding mechanism. The message is identical with its meaning'* (Hofstadter 1979).

658  
659 Chance and Williams (1955; 1956) introduced five classical states of mitochondrial respiration  
660 and cytochrome redox states. **Table 3** shows a protocol with isolated mitochondria in a closed  
661 respirometric chamber, defining a sequence of respiratory states. States and rates are not  
662 distinguished in this nomenclature.

663  
664 **2.6.1. State 1** is obtained after addition of isolated mitochondria to air-saturated  
665 isoosmotic/isotonic respiration medium containing P<sub>i</sub>, but no fuel substrates and no adenylates.

666  
667 **2.6.2. State 2** is induced by addition of a 'high' concentration of ADP (typically 100 to 300 μM),  
668 which stimulates respiration transiently on the basis of endogenous fuel substrates and  
669 phosphorylates only a small portion of the added ADP. State 2 is then obtained at a low respiratory  
670 activity limited by exhausted endogenous fuel substrate availability (**Table 3**). If addition of  
671 specific inhibitors of respiratory complexes such as rotenone does not cause a further decline of  
672 O<sub>2</sub> flux, State 2 is equivalent to the ROX state (**Table 1**). Undefined endogenous fuel substrates are  
673 a confounding factor of pathway control, contributing to the effect of subsequently externally  
674 added substrates and inhibitors. In an alternative sequence of titration steps, the second state is  
675 induced by addition of fuel substrate without ADP or ATP (Estabrook 1967). In contrast to the  
676 original State 2 defined in **Table 1** as a ROX state, the alternative 'State 2' is a LEAK-state with  
677 L(n). Some researchers have called this condition as 'pseudostate 4'.

678  
679 **2.6.3. State 3** is the state stimulated by addition of fuel substrates while the ADP concentration in  
680 the original State 2 is still high (**Table 3**) and supports coupled energy transformation. 'High ADP'  
681 is a concentration of ADP specifically selected to allow the measurement of State 3 to State 4  
682 transitions of isolated mitochondria in a closed respirometric chamber. Repeated ADP titration  
683 re-establishes State 3 at 'high ADP'. Starting at O<sub>2</sub> concentrations near air-saturation (193 or 238  
684 μM O<sub>2</sub> at 37 °C or 25 °C and sea level at 1 atm or 101.32 kPa, and an oxygen solubility of respiration  
685 medium at 0.92 times that of pure water; Forstner and Gnaiger 1983), the total ADP concentration  
686 added must be low enough (typically 100 to 300 μM) to allow phosphorylation to ATP at a coupled  
687 O<sub>2</sub> flux that does not lead to O<sub>2</sub> depletion during the transition to State 4. In contrast, kinetically-  
688 saturating ADP concentrations usually are 10-fold higher than 'high ADP', e.g., 2.5 mM in isolated  
689 mitochondria. The abbreviation State 3u is occasionally used in bioenergetics, to indicate the state  
690 of respiration after titration of an uncoupler, without sufficient emphasis on the fundamental  
691 difference between OXPHOS-capacity (*well-coupled* with an endogenous uncoupled component)  
692 and ET-capacity (*noncoupled*).

693  
694 **2.6.4. State 4** is a LEAK-state that is obtained only if the mitochondrial preparation is intact and  
695 well-coupled. Depletion of ADP by phosphorylation to ATP causes a decline of O<sub>2</sub> flux in the  
696 transition from State 3 to State 4. Under the conditions of State 4, a maximum protonmotive force  
697 and high ATP/ADP ratio are maintained. The gradual decline of Y<sub>P<sub>o</sub>/O<sub>2</sub></sub> towards diminishing [ADP]  
698 at State 4 must be taken into account for calculation of P<sub>o</sub>/O<sub>2</sub> ratios (Gnaiger 2001). State 4  
699 respiration, L(T) (**Table 1**), reflects intrinsic proton leak and ATP hydrolysis activity. O<sub>2</sub> flux in  
700 State 4 is an overestimation of LEAK-respiration if the contaminating ATP hydrolysis activity  
701 recycles some ATP to ADP, J<sub>P<sub>o</sub></sub>, which stimulates respiration coupled to phosphorylation, J<sub>P<sub>o</sub></sub> > 0.  
702 Some degree of mechanical disruption and loss of mitochondrial integrity allows the exposed  
703 mitochondrial F<sub>1</sub>F<sub>0</sub>-ATPases to hydrolyze the ATP synthesized by the fraction of coupled  
704 mitochondria. This can be tested by inhibition of the phosphorylation-pathway using oligomycin,  
705 ensuring that J<sub>P<sub>o</sub></sub> = 0 (State 4o). On the other hand, the State 4 respiration reached after exhaustion

706 of added ADP is a more physiological condition, *i.e.*, presence of ATP, ADP and even AMP.  
707 Sequential ADP titrations re-establish State 3, followed by State 3 to State 4 transitions while  
708 sufficient O<sub>2</sub> is available. Anoxia may be reached, however, before exhaustion of ADP (State 5).

709  
710 **2.6.5. State 5** 'may be obtained by antimycin A treatment or by anaerobiosis' (Chance and Williams,  
711 1955). These definitions give State 5 two different meanings: ROX or anoxia. Anoxia is obtained  
712 after exhaustion of O<sub>2</sub> in a closed respirometric chamber. Diffusion of O<sub>2</sub> from the surroundings  
713 into the aqueous solution may be a confounding factor preventing complete anoxia (Gnaiger  
714 2001).

715 In **Table 3**, only States 3 and 4 are coupling control states, with the restriction that rates in  
716 State 3 may be limited kinetically by non-saturating ADP concentrations.

717  
718 *2.7. Control and regulation*

719  
720 **Reference to Part 1. Quantitative mitochondrial physiology. Mitochondria and bioblasts**

### 721 **3. What is a rate?**

722  
723  
724 The term *rate* is not adequately defined to be useful for reporting data. Normalization of rates  
725 leads to a diversity of formats. Application of common and defined units is required for direct  
726 transfer of reported results into a data repository. The second [s] is the SI unit for the base  
727 quantity *time*. It is also the standard time-unit used in solution chemical kinetics.

728 The inconsistency of the meanings of rate becomes apparent when considering Galileo Galilei's  
729 famous principle, that 'bodies of different weight all fall at the same rate (have a constant  
730 acceleration)' (Coopersmith 2010). A rate may be an extensive quantity, which is a *flow*, *I*, when  
731 expressed per *object* (per number of cells or organisms) or per chamber (per instrumental  
732 system). *System* is defined as the open or closed chamber of the measuring device. A rate is a *flux*,  
733 *J*, when expressed as a size-specific quantity (**Figure 5A; Box 1**).

---

#### 735 **Box 1: Metabolic flows and fluxes: vectorial, vectorial, and scalar**

736  
737 Flow is an extensive quantity (*I*; per system), distinguished from flux as a size-specific quantity (*J*;  
738 per system size). *Flows*, *I*<sub>tr</sub>, are defined for all transformations as extensive quantities. This is a  
739 generalization derived from electrical terms: Electric charge per unit time is electric flow or  
740 current,  $I_{el} = dQ_{el} \cdot dt^{-1}$  [ $A \equiv C \cdot s^{-1}$ ]. When dividing *I*<sub>el</sub> by size of the system (cross-sectional area of a  
741 'wire'), we obtain flux as a size-specific quantity; this is the current density (surface-density of  
742 flow) perpendicular to the direction of flux,  $J_{el} = I_{el} \cdot A^{-1}$  [ $A \cdot m^{-2}$ ] (Cohen *et al* 2008). Fluxes with  
743 *spatial* geometric direction and magnitude are *vectors*. Vector and scalar *fluxes* are related to flows  
744 as  $J_{tr} = I_{tr} \cdot A^{-1}$  [ $mol \cdot s^{-1} \cdot m^{-2}$ ] and  $J_{tr} = I_{tr} \cdot V^{-1}$  [ $mol \cdot s^{-1} \cdot m^{-3}$ ], expressing flux as an area-specific vector or  
745 volume-specific vectorial or scalar quantity, respectively (Gnaiger 1993b). We use the metre-  
746 kilogram-second-ampere (MKSA) international system of units (SI) for general cases ([m], [kg],  
747 [s] and [A]), with decimal SI prefixes for specific applications (**Table 4**).

748 We suggest defining: (1) *vectorial* fluxes, which are translocations as functions of *gradients* with  
749 direction in geometric space in continuous systems; (2) *vectorial* fluxes, which describe  
750 translocations in discontinuous systems and are restricted to information on *compartmental*  
751 *differences* (transmembrane proton flux); and (3) *scalar* fluxes, which are localized  
752 transformations without translocation, such as chemical reactions in a homogenous system  
753 (catabolic O<sub>2</sub> flux, *J*<sub>kO<sub>2</sub></sub>).

---

754  
755 • **Extensive quantities:** An extensive quantity increases proportionally with system size. For  
756 example, mass and volume are extensive quantities. Flow is an extensive quantity. The  
757 magnitude of an extensive quantity is completely additive for non-interacting subsystems. The  
758 magnitude of these quantities depends on the extent or size of the system (Cohen *et al* 2008).

- 759 • **Size-specific quantities:** ‘The adjective *specific* before the name of an extensive quantity is  
 760 often used to mean *divided by mass*’ (Cohen *et al* 2008). The term *specific* has different  
 761 meanings in three particular contexts: (1) In the system-paradigm, (a) mass-specific flux is flow  
 762 divided by mass of the system (the mass of everything contained in the instrumental chamber  
 763 or reactor). (b) Rates are frequently expressed as volume-specific flux (volume of the  
 764 instrumental chamber). A mass-specific or volume-specific quantity is independent of the  
 765 extent of non-interacting homogenous subsystems. (2) In the context of *sample size*, tissue-  
 766 specific quantities are related to the mass or volume of the sample in contrast to the mass or  
 767 volume of the *system* (e.g., muscle mass-specific or cell volume-specific normalization; **Figure**  
 768 **5**). (3) An entirely different meaning is implied in the context of *sample type* (e.g., muscle-  
 769 specific compared to brain-specific properties).
- 770 • **Intensive quantities:** In contrast to size-specific properties, forces are intensive quantities  
 771 defined as the change of an extensive quantity per advancement of an energy transformation  
 772 (Gnaiger 1993b).
- 773 • **Formats:** The quantity of a sample  $X$  can be expressed in different formats.  $n_X$ ,  $N_X$ , and  $m_X$  are  
 774 the molar amount, number, and mass of  $X$ , respectively. When different formats are indicated  
 775 in symbols of derived quantities, the format ( $\underline{n}$ ,  $\underline{N}$ ,  $\underline{m}$ ) is shown as a subscript (*underlined italic*),  
 776 such as in  $I_{O_2/\underline{N}X}$  and  $J_{O_2/\underline{m}X}$ . As of 2019 May 20, the definition of the SI unit mole [mol] is based  
 777 on a natural constant, namely Avogadro’s constant: one mole contains exactly  $6.02214076 \cdot 10^{23}$   
 778 elementary entities, in contrast to the former definition in terms of the number of atoms in the  
 779 mass of 0.012 kilogram of carbon 12 (Gibney 2018). Metabolic oxygen flow and flux are  
 780 expressed in the molar format,  $n_{O_2}$  [mol], but in the volume format,  $V_{O_2}$  [m<sup>3</sup>], in ergometry.  
 781 These formats are distinguished as  $J_{\underline{n}O_2/\underline{m}X}$  and  $J_{V\underline{O}_2/\underline{m}X}$ , respectively, for mass-specific flux.  
 782 Further examples are given in **Table 4** and **Figure 5**.

#### 784 4. Normalization of rate per sample

785  
 786 The challenges of measuring mitochondrial respiratory flux are matched by those of  
 787 normalization. Normalization (**Table 4**) is guided by physicochemical principles, methodological  
 788 considerations, and conceptual strategies (**Figure 5**).

##### 790 4.1. Flow: per object

791  
 792 **4.1.1. Number concentration,  $C_{NX}$ :** Normalization per sample concentration is routinely required  
 793 to report respiratory data.  $C_{NX}$  is the experimental number concentration of sample  $X$ . In the case  
 794 of animals  $N_X$  is the number of organisms in the chamber, e.g., nematodes,  $C_{NX} = N_X \cdot V^{-1}$  [x·L<sup>-1</sup>].  
 795 Similarly, the number of cells per chamber volume is the number concentration of cells,  $C_{Nce} =$   
 796  $N_{ce} \cdot V^{-1}$  [x·L<sup>-1</sup>], where  $N_{ce}$  is the number of cells in the chamber (**Table 4**).

797  
 798 **4.1.2. Flow per object,  $I_{O_2/\underline{N}X}$ :** O<sub>2</sub> flow per cell is calculated from volume-specific O<sub>2</sub> flux,  $J_{V,O_2}$   
 799 [nmol·s<sup>-1</sup>·L<sup>-1</sup>] (per  $V$  of the instrumental chamber [L]), divided by the number concentration of  
 800 cells. The total cell count is the sum of viable and dead cells,  $N_{ce} = N_{vce} + N_{dce}$  (**Table 5**). The cell  
 801 viability index,  $VI = N_{vce} \cdot N_{ce}^{-1}$ , is the ratio of the number of viable cells,  $N_{vce}$ , per total number of  
 802 living cells in the population. After experimental permeabilization, all cells are permeabilized,  $N_{pce}$   
 803  $= N_{ce}$ . The cell viability index can be used to normalize respiration for the number of cells that have  
 804 been viable before experimental permeabilization,  $I_{O_2/\underline{N}vce} = I_{O_2/\underline{N}ce} \cdot VI^{-1}$ , considering that  
 805 mitochondrial respiratory dysfunction in dead cells should be eliminated as a confounding factor.

##### 807 4.2. Size-specific flux: per sample size

808  
 809 **4.2.1. Sample concentration,  $C_{mX}$ :** Considering permeabilized tissue, homogenate or cells as the  
 810 sample,  $X$ , the sample mass is  $m_X$  [mg], which is frequently measured as wet or dry mass,  $m_w$  or  $m_d$  [mg],  
 811 respectively, or as mass of protein,  $m_{\text{Protein}}$ . The sample concentration is the mass of the subsample per

812 volume of the instrumental chamber,  $C_{mX} = m_X \cdot V^{-1}$  [ $\text{g} \cdot \text{L}^{-1} = \text{mg} \cdot \text{mL}^{-1}$ ].  $X$  is the type of sample—isolated  
 813 mitochondria, tissue homogenate, permeabilized muscle fibers or cells (**Table 4**).  $m_{ce}$  [mg] is the total  
 814 mass of all cells in an instrumental chamber, whereas  $m_{Nce} = m_{ce} \cdot N_{ce}^{-1}$  [ $\text{mg} \cdot \text{x}^{-1}$ ] is the (average) mass of  
 815 an individual cell (**Table 5**).

816  
817

818 **4.2.2. Size-specific flux:** Cellular  $\text{O}_2$  flow can be compared between cells of identical size. To take  
 819 into account changes and differences in cell size (Renner *et al* 2003), normalization is required to  
 820 obtain cell size-specific or mitochondrial marker-specific  $\text{O}_2$  flux (**Figure 5**).

821

822 • **Mass-specific flux,  $J_{\text{O}_2/mX}$**  [ $\text{mol} \cdot \text{s}^{-1} \cdot \text{kg}^{-1}$ ]: Mass-specific flux is the expression of respiration per  
 823 mass of sample,  $m_X$  [mg]. Chamber volume-specific flux,  $J_{V,\text{O}_2}$ , is divided by mass concentration  
 824 of  $X$  in the chamber,  $J_{\text{O}_2/mX} = J_{V,\text{O}_2} \cdot C_{mX}^{-1}$ . Cell mass-specific flux is obtained by dividing flow per  
 825 cell by mass per cell,  $J_{\text{O}_2/mce} = I_{\text{O}_2/Nce} \cdot m_{Nce}^{-1}$ .

826 • **Cell volume-specific flux,  $J_{\text{O}_2/VX}$**  [ $\text{mol} \cdot \text{s}^{-1} \cdot \text{m}^{-3}$ ]: Sample volume-specific flux is obtained by  
 827 expressing respiration per volume of sample.

828

829 If size-specific  $\text{O}_2$  flux is constant and independent of sample size, then there is no interaction  
 830 between the subsystems. For example, 1.5 mg and 3.0 mg sub-samples of muscle tissue respire at  
 831 identical mass-specific flux. If mass-specific  $\text{O}_2$  flux, however, changes as a function of the mass of  
 832 a tissue sample, cells or isolated mitochondria in the instrumental chamber, then the nature of the  
 833 interaction becomes an issue. Therefore, cell concentration must be optimized, particularly in  
 834 experiments carried out in wells, considering the confluency of the cell monolayer or clumps of  
 835 cells (Salabei *et al* 2014).

836 The complexity changes when considering the scaling law of respiratory physiology. Strong  
 837 interactions are revealed between  $\text{O}_2$  flow and body mass of an individual organism: *basal*  
 838 metabolic rate (flow) does not increase linearly with body mass, whereas *maximum* mass-specific  
 839  $\text{O}_2$  flux,  $\dot{V}_{\text{O}_2\text{max}}$  or  $\dot{V}_{\text{O}_2\text{peak}}$ , is approximately constant across a large range of individual body mass  
 840 (Weibel and Hoppeler 2005). Individuals, breeds and species, however, deviate substantially from  
 841 this relationship.  $\dot{V}_{\text{O}_2\text{peak}}$  of human endurance athletes is 60 to 80  $\text{mL O}_2 \cdot \text{min}^{-1} \cdot \text{kg}^{-1}$  body mass,  
 842 converted to  $J_{\text{O}_2\text{peak}/m\text{Norg}}$  of 45 to 60  $\text{nmol} \cdot \text{s}^{-1} \cdot \text{g}^{-1}$  (Gnaiger 2020; **Table 6**).

843

844 *4.3. Marker-specific flux: per mitochondrial content*

845

846 **Reference to Part 3. Quantitative mitochondrial physiology. Mitochondrial markers**

847

## 848 5. Normalization of rate per system

849

### 850 5.1. Flow: per chamber

851

852 The instrumental system (chamber) is part of the measurement instrument, separated from the  
 853 environment as an isolated, closed, open, isothermal or non-isothermal system (**Table 4**).  
 854 Reporting  $\text{O}_2$  flows per respiratory chamber,  $I_{\text{O}_2}$  [ $\text{nmol} \cdot \text{s}^{-1}$ ], restricts the analysis to intra-  
 855 experimental comparison of relative differences.

856

### 857 5.2. Flux: per chamber volume

858

859 **5.2.1. System-specific flux,  $J_{V,\text{O}_2}$ :** We distinguish between (1) the *system* with volume  $V$  and mass  
 860  $m$  defined by the system boundaries, and (2) the *sample* or *objects* with volume  $V_X$  and mass  $m_X$   
 861 that are enclosed in the instrumental chamber (**Figure 5**). Metabolic  $\text{O}_2$  flow per object,  $I_{\text{O}_2/NX}$ , is  
 862 the total  $\text{O}_2$  flow in the system divided by the number of objects,  $N_X$ , in the system.  $I_{\text{O}_2/NX}$  increases  
 863 as the mass of the object is increased. Sample mass-specific  $\text{O}_2$  flux,  $J_{\text{O}_2/mX}$  should be independent



864 of the mass-concentration of the subsample obtained from the same tissue or cell culture, but  
 865 system volume-specific O<sub>2</sub> flux,  $J_{V,O_2}$  (per liquid volume of the instrumental chamber), increases in  
 866 proportion to the mass of the sample in the chamber. Although  $J_{V,O_2}$  depends on mass-  
 867 concentration of the sample in the chamber, it should be independent of the chamber (system)  
 868 volume at constant sample mass- concentration. There are practical limitations to increasing the  
 869 mass-concentration of the sample in the chamber, when one is concerned about crowding effects  
 870 and instrumental time resolution. The wall of the chamber and the enclosed solid stirrer are not  
 871 counted as part of the chamber volume.

872  
 873 **5.2.2. Advancement per volume:** When the reactor volume does not change during the reaction,  
 874 which is typical for liquid phase reactions, the volume-specific flux of a chemical reaction  $r$  is the  
 875 time derivative of the advancement of the reaction per unit volume,  $J_{V,rB} = d_r \xi_B / dt \cdot V^{-1}$  [(mol·s<sup>-1</sup>)·L<sup>-1</sup>].  
 876 The rate of concentration change is  $dc_B / dt$  [(mol·L<sup>-1</sup>)·s<sup>-1</sup>], where concentration is  $c_B = n_B \cdot V^{-1}$ . There  
 877 is a difference between (1)  $J_{V,rO_2}$  [mol·s<sup>-1</sup>·L<sup>-1</sup>] and (2) rate of concentration change [mol·L<sup>-1</sup>·s<sup>-1</sup>].  
 878 These merge into a single expression only in closed systems. In open systems, internal  
 879 transformations (catabolic flux, O<sub>2</sub> consumption) are distinguished from external flux (such as O<sub>2</sub>  
 880 supply). External fluxes of all substances are zero in closed systems. In a closed chamber O<sub>2</sub>  
 881 consumption (internal flux of catabolic reactions  $k$ ;  $I_{kO_2}$  [pmol·s<sup>-1</sup>]) causes a decline in the amount  
 882 of O<sub>2</sub> in the system,  $n_{O_2}$  [nmol]. Normalization of these quantities for the volume of the system,  $V$   
 883 [L  $\equiv$  dm<sup>3</sup>], yields volume-specific O<sub>2</sub> flux,  $J_{V,kO_2} = I_{kO_2} / V$  [nmol·s<sup>-1</sup>·L<sup>-1</sup>], and O<sub>2</sub> concentration, [O<sub>2</sub>] or  
 884  $c_{O_2} = n_{O_2} \cdot V^{-1}$  [ $\mu$ mol·L<sup>-1</sup> =  $\mu$ M = nmol·mL<sup>-1</sup>]. Instrumental background O<sub>2</sub> flux is due to external flux  
 885 into a non-ideal closed respirometer, so total volume-specific flux has to be corrected for  
 886 instrumental background O<sub>2</sub> flux—O<sub>2</sub> diffusion into or out of the instrumental chamber.  $J_{V,kO_2}$  is  
 887 relevant mainly for methodological reasons and should be compared with the accuracy of  
 888 instrumental resolution of background-corrected flux, e.g.,  $\pm 1$  nmol·s<sup>-1</sup>·L<sup>-1</sup> (Gnaiger 2001).  
 889 ‘Catabolic’ indicates O<sub>2</sub> flux,  $J_{kO_2}$ , corrected for: (1) instrumental background O<sub>2</sub> flux; (2) chemical  
 890 background O<sub>2</sub> flux due to autoxidation of chemical components added to the incubation medium;  
 891 and (3) *Rox* for O<sub>2</sub>-consuming side reactions unrelated to the catabolic pathway  $k$ .

## 892 6. Conversion of units

893  
 894  
 895 Many different units have been used to report the O<sub>2</sub> consumption rate, OCR (Table 6). SI base  
 896 units provide the common reference to introduce the theoretical principles (Figure 5), and are  
 897 used with appropriately chosen SI prefixes to express numerical data in the most practical format,  
 898 with an effort towards unification within specific areas of application (Table 7). Reporting data  
 899 in SI units—including the mole [mol], coulomb [C], joule [J], and second [s]—should be  
 900 encouraged, particularly by journals that propose the use of SI units.

901 Although volume is expressed as m<sup>3</sup> using the SI base unit, the litre [dm<sup>3</sup>] is a conventional unit  
 902 of volume for concentration and is used for most solution chemical kinetics. If one multiplies  $I_{O_2/Nce}$   
 903 by  $C_{Nce}$ , then the result will not only be the amount of O<sub>2</sub> [mol] consumed per time [s<sup>-1</sup>] in one litre  
 904 [L<sup>-1</sup>], but also the change in O<sub>2</sub> concentration per second (for any volume of an ideally closed  
 905 system). This is ideal for kinetic modeling as it blends with chemical rate equations where  
 906 concentrations are typically expressed in mol·L<sup>-1</sup> (Wagner *et al* 2011). In studies of multinuclear  
 907 cells—such as differentiated skeletal muscle cells—it is easy to determine the number of nuclei  
 908 but not the total number of cells. A generalized concept, therefore, is obtained by substituting cells  
 909 by nuclei as the sample entity. This does not hold, however, for non-nucleated platelets.

910 For studies of cells, we recommend that respiration be expressed, as far as possible, as: (1) O<sub>2</sub>  
 911 flux normalized for a mitochondrial marker, for separation of the effects of mitochondrial quality  
 912 and content on cell respiration (this includes *FCRs* as a normalization for a functional  
 913 mitochondrial marker); (2) O<sub>2</sub> flux in units of cell volume or mass, for comparison of respiration  
 914 of cells with different cell size (Renner *et al* 2003) and with studies on tissue preparations, and  
 915 (3) O<sub>2</sub> flow in units of attomole (10<sup>-18</sup> mol) of O<sub>2</sub> consumed per second by each cell [amol·s<sup>-1</sup>·cell

916 <sup>1</sup>], numerically equivalent to [ $\text{pmol}\cdot\text{s}^{-1}\cdot 10^{-6}$  cells]. This convention allows information to be easily  
917 used when designing experiments in which  $\text{O}_2$  flow must be considered. For example, to estimate  
918 the volume-specific  $\text{O}_2$  flux in an instrumental chamber that would be expected at a particular cell  
919 number concentration, one simply needs to multiply the flow per cell by the number of cells per  
920 volume of interest. This provides the amount of  $\text{O}_2$  [mol] consumed per time [ $\text{s}^{-1}$ ] per unit volume  
921 [ $\text{L}^{-1}$ ]. At an  $\text{O}_2$  flow of  $100 \text{ amol}\cdot\text{s}^{-1}\cdot\text{cell}^{-1}$  and a cell concentration of  $10^9 \text{ cells}\cdot\text{L}^{-1}$  ( $10^6 \text{ cells}\cdot\text{mL}^{-1}$ ), the  
922 volume-specific  $\text{O}_2$  flux is  $100 \text{ nmol}\cdot\text{s}^{-1}\cdot\text{L}^{-1}$  ( $100 \text{ pmol}\cdot\text{s}^{-1}\cdot\text{mL}^{-1}$ ).

923 ET-capacity in human cell types including HEK 293, primary HUVEC, and fibroblasts ranges  
924 from 50 to  $180 \text{ amol}\cdot\text{s}^{-1}\cdot\text{cell}^{-1}$ , measured in living cells in the noncoupled state (Gnaiger 2020). At  
925  $100 \text{ amol}\cdot\text{s}^{-1}\cdot\text{cell}^{-1}$  corrected for *Rox*, the current across the mt- membranes,  $I_{\text{H}^+e}$ , approximates  
926  $193 \text{ pA}\cdot\text{cell}^{-1}$  or  $0.2 \text{ nA}$  per cell. See Rich (2003) for an extension of quantitative bioenergetics from  
927 the molecular to the human scale, with a transmembrane proton flux equivalent to  $520 \text{ A}$  in an  
928 adult at a catabolic power of  $-110 \text{ W}$ . Modelling approaches illustrate the link between  
929 protonmotive force and currents (Willis *et al* 2016).

930 We consider isolated mitochondria as powerhouses and proton pumps as molecular machines  
931 to relate experimental results to energy metabolism of living cells. The cellular  $\text{P}\gg/\text{O}_2$  based on  
932 oxidation of glycogen is increased by the glycolytic (fermentative) substrate-level  
933 phosphorylation of  $3 \text{ P}\gg/\text{Glyc}$  or  $0.5 \text{ mol P}\gg$  for each mol  $\text{O}_2$  consumed in the complete oxidation  
934 of a mol glycosyl unit (Glyc). Adding 0.5 to the mitochondrial  $\text{P}\gg/\text{O}_2$  ratio of 5.4 yields a  
935 bioenergetic cell physiological  $\text{P}\gg/\text{O}_2$  ratio close to 6. Two NADH equivalents are formed during  
936 glycolysis and transported from the cytosol into the mitochondrial matrix, either by the malate-  
937 aspartate shuttle or by the glycerophosphate shuttle (Figure 1a) resulting in different theoretical  
938 yields of ATP generated by mitochondria, the energetic cost of which potentially must be taken  
939 into account. Considering also substrate-level phosphorylation in the TCA cycle, this high  $\text{P}\gg/\text{O}_2$   
940 ratio not only reflects proton translocation and OXPHOS studied in isolation, but integrates  
941 mitochondrial physiology with energy transformation in the living cell (Gnaiger 1993a).

942

## 943 7. Conclusions

944

945 Catabolic cell respiration is the process of exergonic and exothermic energy transformation in  
946 which scalar redox reactions are coupled to vectorial ion translocation across a semipermeable  
947 membrane, which separates the small volume of a bacterial cell or mitochondrion from the larger  
948 volume of its surroundings. The electrochemical exergy can be partially conserved in the  
949 phosphorylation of ADP to ATP or in ion pumping, or dissipated in an electrochemical short-  
950 circuit. Respiration is thus clearly distinguished from fermentation as the counterparts of cellular  
951 core energy metabolism. An  $\text{O}_2$  flux balance scheme illustrates the relationships and general  
952 definitions (Figures 1 and 2).

953

---

### 954 Box 2: Recommendations for studies with mitochondrial preparations

955

- 956 • Normalization of respiratory rates should be provided as far as possible:

957

#### 958 A. Sample normalization

959

- 959 1. *Object-specific biophysical normalization*: on a per organism or per cell basis as  $\text{O}_2$  flow; this  
960 may not be possible when dealing with coenocytic organisms, *e.g.*, filamentous fungi, or tissues  
961 without cross-walls separating individual cells, *e.g.*, muscle fibers.
- 962 2. *Size-specific cellular normalization*: per g protein; per organism-, cell- or tissue-mass as mass-  
963 specific  $\text{O}_2$  flux; per cell volume as cell volume-specific flux.
- 964 3. *Mitochondrial normalization*: per mitochondrial marker as mt-specific flux.

965

#### 966 B. Chamber normalization

967

- 967 1. Chamber volume-specific flux,  $J_V$  [ $\text{pmol}\cdot\text{s}^{-1}\cdot\text{mL}^{-1}$ ], is reported for quality control in relation to  
968 instrumental sensitivity and limit of detection of volume-specific flux.

- 969 2. Sample concentration in the instrumental chamber is reported as number concentration, mass  
970 concentration, or mitochondrial concentration; this is a component of the measuring  
971 conditions. With information on cell size and the use of multiple normalizations, maximum  
972 potential information is available (Renner *et al* 2003; Wagner *et al* 2011; Gnaiger 2020).  
973 Reporting flow in a respiratory chamber [ $\text{nmol}\cdot\text{s}^{-1}$ ] is discouraged, since it restricts the analysis  
974 to intra-experimental comparison of relative (qualitative) differences.
- 975 • Catabolic mitochondrial respiration is distinguished from residual  $\text{O}_2$  consumption. Fluxes in  
976 mitochondrial coupling states should be, as far as possible, corrected for residual  $\text{O}_2$   
977 consumption.
  - 978 • Different mechanisms of uncoupling should be distinguished by defined terms. The tightness  
979 of coupling relates to these uncoupling mechanisms, whereas the coupling stoichiometry  
980 varies as a function the substrate type involved in ET-pathways with either three or two redox  
981 proton pumps operating in series. Separation of tightness of coupling from the pathway-  
982 dependent coupling stoichiometry is possible only when the substrate type undergoing  
983 oxidation remains the same for respiration in LEAK-, OXPHOS-, and ET-states. In studies of the  
984 tightness of coupling, therefore, simple substrate-inhibitor combinations should be applied to  
985 exclude a shift in substrate competition that may occur when providing physiological substrate  
986 cocktails.
  - 987 • In studies of isolated mitochondria, the mitochondrial recovery and yield should be reported.  
988 Experimental criteria such as transmission electron microscopy for evaluation of purity versus  
989 integrity should be considered. Mitochondrial markers—such as citrate synthase activity as an  
990 enzymatic matrix marker—provide a link to the tissue of origin on the basis of calculating the  
991 mitochondrial recovery, *i.e.*, the fraction of mitochondrial marker obtained from a unit mass of  
992 tissue. Total mitochondrial protein is frequently applied as a mitochondrial marker, which is  
993 restricted to isolated mitochondria.
  - 994 • In studies of permeabilized cells, the viability of the cell culture or cell suspension of origin  
995 should be reported. Normalization should be evaluated for total cell count or viable cell count.
  - 996 • Terms and symbols are summarized in **Table 8**. Their use will facilitate transdisciplinary  
997 communication and support further development of a consistent theory of bioenergetics and  
998 mitochondrial physiology. Technical terms related to and defined with normal words can be  
999 used as index terms in data repositories, support the creation of ontologies towards semantic  
1000 information processing (MitoPedia), and help in communicating analytical findings as  
1001 impactful data-driven stories. *'Making data available without making it understandable may be  
1002 worse than not making it available at all'* (National Academies of Sciences, Engineering, and  
1003 Medicine 2018). Success will depend on taking further steps: (1) exhaustive text-mining  
1004 considering Omics data and functional data; (2) network analysis of Omics data with  
1005 bioinformatics tools; (3) cross-validation with distinct bioinformatics approaches; (4)  
1006 correlation with physiological data; (5) guidelines for biological validation of network data.  
1007 This is a call to carefully contribute to FAIR principles (Findable, Accessible, Interoperable,  
1008 Reusable) for the sharing of scientific data.

1009  
1010 Experimentally, respiration is separated in mitochondrial preparations from the interactions  
1011 with the fermentative pathways of the living cell. OXPHOS analysis is based on the study of  
1012 mitochondrial preparations complementary to bioenergetic investigations of (1)  
1013 submitochondrial particles and molecular structures, (2) living cells, and (3) organisms—from  
1014 model organisms to the human species including healthy and diseased persons (patients).  
1015 Different mechanisms of respiratory uncoupling have to be distinguished (**Figure 3**). Metabolic  
1016 fluxes measured in defined coupling and pathway control states (**Figures 5 and 6**) provide  
1017 insights into the meaning of cellular and organismic respiration.

1018 The optimal choice for expressing mitochondrial and cell respiration as  $\text{O}_2$  flow per biological  
1019 sample, and normalization for specific tissue-markers (volume, mass, protein) and mitochondrial  
1020 markers (volume, protein, content, mtDNA, activity of marker enzymes, respiratory reference  
1021 state) is guided by the scientific question under study. Interpretation of the data depends critically  
1022 on appropriate normalization (**Figure 5**).

1023 MitoEAGLE can serve as a gateway to better diagnose mitochondrial respiratory adaptations  
1024 and defects linked to genetic variation, age-related health risks, sex-specific mitochondrial  
1025 performance, lifestyle with its effects on degenerative diseases, and thermal and chemical  
1026 environment. The present recommendations on coupling control states and rates are focused on  
1027 studies using mitochondrial preparations (**Box 2**). These will be extended in a series of reports on  
1028 pathway control of mitochondrial respiration, respiratory states and rates in living cells,  
1029 respiratory flux control ratios, and harmonization of experimental procedures.  
1030

## 1031 References

- 1032  
1033 Altmann R (1894) Die Elementarorganismen und ihre Beziehungen zu den Zellen. Zweite vermehrte  
1034 Auflage. Verlag Von Veit & Comp, Leipzig:160 pp.  
1035 Baggeto LG, Testa-Perussini R (1990) Role of acetoin on the regulation of intermediate metabolism of  
1036 Ehrlich ascites tumor mitochondria: its contribution to membrane cholesterol enrichment modifying  
1037 passive proton permeability. Arch Biochem Biophys 283:341-8.  
1038 Beard DA (2005) A biophysical model of the mitochondrial respiratory system and oxidative  
1039 phosphorylation. PLoS Comput Biol 1(4):e36.  
1040 Benda C (1898) Weitere Mitteilungen über die Mitochondria. Verh Dtsch Physiol Ges:376-83.  
1041 Birkedal R, Laasmaa M, Vendelin M (2014) The location of energetic compartments affects energetic  
1042 communication in cardiomyocytes. Front Physiol 5:376.  
1043 Blier PU, Dufresne F, Burton RS (2001) Natural selection and the evolution of mtDNA-encoded peptides:  
1044 evidence for intergenomic co-adaptation. Trends Genet 17:400-6.  
1045 Blier PU, Guderley HE (1993) Mitochondrial activity in rainbow trout red muscle: the effect of temperature  
1046 on the ADP-dependence of ATP synthesis. J Exp Biol 176:145-58.  
1047 Breton S, Beaupré HD, Stewart DT, Hoeh WR, Blier PU (2007) The unusual system of doubly uniparental  
1048 inheritance of mtDNA: isn't one enough? Trends Genet 23:465-74.  
1049 Brown GC (1992) Control of respiration and ATP synthesis in mammalian mitochondria and cells. Biochem  
1050 J 284:1-13.  
1051 Burger G, Gray MW, Forget L, Lang BF (2013) Strikingly bacteria-like and gene-rich mitochondrial genomes  
1052 throughout jakobid protists. Genome Biol Evol 5:418-38.  
1053 Calvo SE, Klauser CR, Mootha VK (2016) MitoCarta2.0: an updated inventory of mammalian mitochondrial  
1054 proteins. Nucleic Acids Research 44:D1251-7.  
1055 Calvo SE, Julien O, Clauser KR, Shen H, Kamer KJ, Wells JA, Mootha VK (2017) Comparative analysis of  
1056 mitochondrial N-termini from mouse, human, and yeast. Mol Cell Proteomics 16:512-23.  
1057 Campos JC, Queliconi BB, Bozi LHM, Bechara LRG, Dourado PMM, Andres AM, Jannig PR, Gomes KMS,  
1058 Zambelli VO, Rocha-Resende C, Guatimosim S, Brum PC, Mochly-Rosen D, Gottlieb RA, Kowaltowski AJ,  
1059 Ferreira JCB (2017) Exercise reestablishes autophagic flux and mitochondrial quality control in heart  
1060 failure. Autophagy 13:1304-317.  
1061 Canton M, Luvisetto S, Schmehl I, Azzone GF (1995) The nature of mitochondrial respiration and  
1062 discrimination between membrane and pump properties. Biochem J 310:477-81.  
1063 Carrico C, Meyer JG, He W, Gibson BW, Verdin E (2018) The mitochondrial acylome emerges: proteomics,  
1064 regulation by Sirtuins, and metabolic and disease implications. Cell Metab 27:497-512.  
1065 Chan DC (2006) Mitochondria: dynamic organelles in disease, aging, and development. Cell 125:1241-52.  
1066 Chance B, Williams GR (1955a) Respiratory enzymes in oxidative phosphorylation. I. Kinetics of oxygen  
1067 utilization. J Biol Chem 217:383-93.  
1068 Chance B, Williams GR (1955b) Respiratory enzymes in oxidative phosphorylation: III. The steady state. J  
1069 Biol Chem 217:409-27.  
1070 Chance B, Williams GR (1955c) Respiratory enzymes in oxidative phosphorylation. IV. The respiratory  
1071 chain. J Biol Chem 217:429-38.  
1072 Chance B, Williams GR (1956) The respiratory chain and oxidative phosphorylation. Adv Enzymol Relat  
1073 Subj Biochem 17:65-134.  
1074 Chowdhury SK, Djordjevic J, Albensi B, Fernyhough P (2015) Simultaneous evaluation of substrate-  
1075 dependent oxygen consumption rates and mitochondrial membrane potential by TMRM and safranin in  
1076 cortical mitochondria. Biosci Rep 36:e00286.  
1077 Cobb LJ, Lee C, Xiao J, Yen K, Wong RG, Nakamura HK, Mehta HH, Gao Q, Ashur C, Huffman DM, Wan J,  
1078 Muzumdar R, Barzilai N, Cohen P (2016) Naturally occurring mitochondrial-derived peptides are age-  
1079 dependent regulators of apoptosis, insulin sensitivity, and inflammatory markers. Aging (Albany NY)  
1080 8:796-809.



- 1081 Cohen ER, Cvitas T, Frey JG, Holmström B, Kuchitsu K, Marquardt R, Mills I, Pavese F, Quack M, Stohner J,  
1082 Strauss HL, Takami M, Thor HL (2008) Quantities, units and symbols in physical chemistry, IUPAC Green  
1083 Book, 3rd Edition, 2nd Printing, IUPAC & RSC Publishing, Cambridge.
- 1084 Cooper H, Hedges LV, Valentine JC, eds (2009) The handbook of research synthesis and meta-analysis.  
1085 Russell Sage Foundation.
- 1086 Coopersmith J (2010) Energy, the subtle concept. The discovery of Feynman's blocks from Leibnitz to  
1087 Einstein. Oxford University Press:400 pp.
- 1088 Cummins J (1998) Mitochondrial DNA in mammalian reproduction. Rev Reprod 3:172-82.
- 1089 Dai Q, Shah AA, Garde RV, Yonish BA, Zhang L, Medvitz NA, Miller SE, Hansen EL, Dunn CN, Price TM (2013)  
1090 A truncated progesterone receptor (PR-M) localizes to the mitochondrion and controls cellular  
1091 respiration. Mol Endocrinol 27:741-53.
- 1092 Daum B, Walter A, Horst A, Osiewacz HD, Kühlbrandt W (2013) Age-dependent dissociation of ATP synthase  
1093 dimers and loss of inner-membrane cristae in mitochondria. Proc Natl Acad Sci U S A 110:15301-6.
- 1094 Diebold LP, Gil HJ, Gao P, Martinez CA, Weinberg SE, Chandel NS (2019) Mitochondrial Complex III is  
1095 necessary for endothelial cell proliferation during angiogenesis. Nat Metab 1:158-71.
- 1096 Divakaruni AS, Brand MD (2011) The regulation and physiology of mitochondrial proton leak. Physiology  
1097 (Bethesda) 26:192-205.
- 1098 Doerrier C, Garcia-Souza LF, Krumschnabel G, Wohlfarter Y, Mészáros AT, Gnaiger E (2018) High-Resolution  
1099 FluoRespirometry and OXPHOS protocols for human cells, permeabilized fibres from small biopsies of  
1100 muscle, and isolated mitochondria. Methods Mol Biol 1782 (Palmeira CM, Moreno AJ, eds):  
1101 Mitochondrial Bioenergetics, 978-1-4939-7830-4.
- 1102 Doskey CM, van 't Erve TJ, Wagner BA, Buettner GR (2015) Moles of a substance per cell is a highly  
1103 informative dosing metric in cell culture. PLoS One 10:e0132572.
- 1104 Drahota Z, Milerová M, Stieglerová A, Houstek J, Ostádal B (2004) Developmental changes of cytochrome c  
1105 oxidase and citrate synthase in rat heart homogenate. Physiol Res 53:119-22.
- 1106 Duarte FV, Palmeira CM, Rolo AP (2014) The role of microRNAs in mitochondria: small players acting wide.  
1107 Genes (Basel) 5:865-86.
- 1108 Ehinger JK, Morota S, Hansson MJ, Paul G, Elmér E (2015) Mitochondrial dysfunction in blood cells from  
1109 amyotrophic lateral sclerosis patients. J Neurol 262:1493-503.
- 1110 Ehinger JK, Piel S, Ford R, Karlsson M, Sjövall F, Frostner EÅ, Morota S, Taylor RW, Turnbull DM, Cornell C,  
1111 Moss SJ, Metzsch C, Hansson MJ, Fliri H, Elmér E (2016) Cell-permeable succinate prodrugs bypass  
1112 mitochondrial complex I deficiency. Nat Commun 7:12317.
- 1113 Ernster L, Schatz G (1981) Mitochondria: a historical review. J Cell Biol 91:227s-55s.
- 1114 Estabrook RW (1967) Mitochondrial respiratory control and the polarographic measurement of ADP:O  
1115 ratios. Methods Enzymol 10:41-7.
- 1116 Faber C, Zhu ZJ, Castellino S, Wagner DS, Brown RH, Peterson RA, Gates L, Barton J, Bickett M, Hagerty L,  
1117 Kimbrough C, Sola M, Bailey D, Jordan H, Elangbam CS (2014) Cardiolipin profiles as a potential  
1118 biomarker of mitochondrial health in diet-induced obese mice subjected to exercise, diet-restriction and  
1119 ephedrine treatment. J Appl Toxicol 34:1122-9.
- 1120 Feagin JE, Harrell MI, Lee JC, Coe KJ, Sands BH, Cannone JJ, Tami G, Schnare MN, Gutell RR (2012) The  
1121 fragmented mitochondrial ribosomal RNAs of *Plasmodium falciparum*. PLoS One 7:e38320.
- 1122 Fell D (1997) Understanding the control of metabolism. Portland Press.
- 1123 Forstner H, Gnaiger E (1983) Calculation of equilibrium oxygen concentration. In: Polarographic Oxygen  
1124 Sensors. Aquatic and Physiological Applications. Gnaiger E, Forstner H (eds), Springer, Berlin,  
1125 Heidelberg, New York:321-33.
- 1126 Garlid KD, Beavis AD, Ratkje SK (1989) On the nature of ion leaks in energy-transducing membranes.  
1127 Biochim Biophys Acta 976:109-20.
- 1128 Garlid KD, Semrad C, Zinchenko V. Does redox slip contribute significantly to mitochondrial respiration? In:  
1129 Schuster S, Rigoulet M, Ouhabi R, Mazat J-P, eds (1993) Modern trends in biothermokinetics. Plenum  
1130 Press, New York, London:287-93.
- 1131 Gebert N, Joshi AS, Kutik S, Becker T, McKenzie M, Guan XL, Mooga VP, Stroud DA, Kulkarni G, Wenk MR,  
1132 Rehling P, Meisinger C, Ryan MT, Wiedemann N, Greenberg ML, Pfanner N (2009) Mitochondrial  
1133 cardiolipin involved in outer-membrane protein biogenesis: implications for Barth syndrome. Curr Biol  
1134 19:2133-9.
- 1135 Gerö D, Szabo C (2016) Glucocorticoids suppress mitochondrial oxidant production via upregulation of  
1136 uncoupling protein 2 in hyperglycemic endothelial cells. PLoS One 11:e0154813.
- 1137 Gibney E (2018) Largest overhaul of scientific units since 1875 wins approval. Nature 563:451-2.  
1138 <https://www.nature.com/articles/d41586-018-07424-8>
- 1139 Gnaiger E (1993a). Efficiency and power strategies under hypoxia. Is low efficiency at high glycolytic ATP  
1140 production a paradox? In: Surviving Hypoxia: Mechanisms of Control and Adaptation. Hochachka PW,

- 1141 Lutz PL, Sick T, Rosenthal M, Van den Thillart G, eds. CRC Press, Boca Raton, Ann Arbor, London,  
1142 Tokyo:77-109.
- 1143 Gnaiger E (1993b) Nonequilibrium thermodynamics of energy transformations. *Pure Appl Chem* 65:1983-  
1144 2002.
- 1145 Gnaiger E (2001) Bioenergetics at low oxygen: dependence of respiration and phosphorylation on oxygen  
1146 and adenosine diphosphate supply. *Respir Physiol* 128:277-97.
- 1147 Gnaiger E (2009) Capacity of oxidative phosphorylation in human skeletal muscle. New perspectives of  
1148 mitochondrial physiology. *Int J Biochem Cell Biol* 41:1837-45.
- 1149 Gnaiger E (2020) Mitochondrial pathways and respiratory control. An introduction to OXPHOS analysis. 5th  
1150 ed. *Bioenerg Commun* 2020.2.
- 1151 Gnaiger E, Aasander Frostner E, Abdul Karim N, Abdel-Rahman EA, Abumrad NA, Acuna-Castroviejo D,  
1152 Adele RC, et al (2020) Mitochondrial respiratory states and rates. *Nat Metab* (in review)
- 1153 Gnaiger E, Méndez G, Hand SC (2000) High phosphorylation efficiency and depression of uncoupled  
1154 respiration in mitochondria under hypoxia. *Proc Natl Acad Sci USA* 97:11080-5.
- 1155 Greggio C, Jha P, Kulkarni SS, Lagarrigue S, Broskey NT, Boutant M, Wang X, Conde Alonso S, Ofori E, Auwerx  
1156 J, Cantó C, Amati F (2017) Enhanced respiratory chain supercomplex formation in response to exercise  
1157 in human skeletal muscle. *Cell Metab* 25:301-11.
- 1158 Hinkle PC (2005) P/O ratios of mitochondrial oxidative phosphorylation. *Biochim Biophys Acta* 1706:1-11.
- 1159 Hofstadter DR (1979) Gödel, Escher, Bach: An eternal golden braid. A metaphorical fugue on minds and  
1160 machines in the spirit of Lewis Carroll. Harvester Press:499 pp.
- 1161 Illaste A, Laasmaa M, Peterson P, Vendelin M (2012) Analysis of molecular movement reveals latticelike  
1162 obstructions to diffusion in heart muscle cells. *Biophys J* 102:739-48.
- 1163 Jasienski M, Bazzaz FA (1999) The fallacy of ratios and the testability of models in biology. *Oikos* 84:321-  
1164 26.
- 1165 Jephthina N, Beraud N, Sepp M, Birkedal R, Vendelin M (2011) Permeabilized rat cardiomyocyte response  
1166 demonstrates intracellular origin of diffusion obstacles. *Biophys J* 101:2112-21.
- 1167 Jezek P, Holendova B, Garlid KD, Jaburek M (2018) Mitochondrial uncoupling proteins: subtle regulators of  
1168 cellular redox signaling. *Antioxid Redox Signal* 29:667-714.
- 1169 Karnkowska A, Vacek V, Zubáčová Z, Treitl SC, Petrželková R, Eme L, Novák L, Žárský V, Barlow LD, Herman  
1170 EK, Soukal P, Hroudová M, Doležal P, Stairs CW, Roger AJ, Eliáš M, Dacks JB, Vlček Č, Hampl V (2016) A  
1171 eukaryote without a mitochondrial organelle. *Curr Biol* 26:1274-84.
- 1172 Kenwood BM, Weaver JL, Bajwa A, Poon IK, Byrne FL, Murrow BA, Calderone JA, Huang L, Divakaruni AS,  
1173 Tomsig JL, Okabe K, Lo RH, Cameron Coleman G, Columbus L, Yan Z, Saucerman JJ, Smith JS, Holmes JW,  
1174 Lynch KR, Ravichandran KS, Uchiyama S, Santos WL, Rogers GW, Okusa MD, Bayliss DA, Hoehn KL (2013)  
1175 Identification of a novel mitochondrial uncoupler that does not depolarize the plasma membrane. *Mol*  
1176 *Metab* 3:114-23.
- 1177 Klepinin A, Ounpuu L, Guzun R, Chekulayev V, Timohhina N, Tepp K, Shevchuk I, Schlattner U, Kaambre T  
1178 (2016) Simple oxygraphic analysis for the presence of adenylate kinase 1 and 2 in normal and tumor  
1179 cells. *J Bioenerg Biomembr* 48:531-48.
- 1180 Koit A, Shevchuk I, Ounpuu L, Klepinin A, Chekulayev V, Timohhina N, Tepp K, Puurand M, Truu L, Heck K,  
1181 Valvere V, Guzun R, Kaambre T (2017) Mitochondrial respiration in human colorectal and breast cancer  
1182 clinical material is regulated differently. *Oxid Med Cell Longev* 1372640.
- 1183 Komlódi T, Tretter L (2017) Methylene blue stimulates substrate-level phosphorylation catalysed by  
1184 succinyl-CoA ligase in the citric acid cycle. *Neuropharmacology* 123:287-98.
- 1185 Korn E (1969) Cell membranes: structure and synthesis. *Annu Rev Biochem* 38:263-88.
- 1186 Lai N, M Kummitha C, Rosca MG, Fujioka H, Tandler B, Hoppel CL (2018) Isolation of mitochondrial  
1187 subpopulations from skeletal muscle: optimizing recovery and preserving integrity. *Acta Physiol*  
1188 (Oxf):e13182. doi: 10.1111/apha.13182.
- 1189 Lane N (2005) Power, sex, suicide: mitochondria and the meaning of life. Oxford University Press:354 pp.
- 1190 Larsen S, Nielsen J, Neigaard Nielsen C, Nielsen LB, Wibrand F, Stride N, Schroder HD, Boushel RC, Helge JW,  
1191 Dela F, Hey-Mogensen M (2012) Biomarkers of mitochondrial content in skeletal muscle of healthy  
1192 young human subjects. *J Physiol* 590:3349-60.
- 1193 Lee C, Zeng J, Drew BG, Sallam T, Martin-Montalvo A, Wan J, Kim SJ, Mehta H, Hevener AL, de Cabo R, Cohen  
1194 P (2015) The mitochondrial-derived peptide MOTS-c promotes metabolic homeostasis and reduces  
1195 obesity and insulin resistance. *Cell Metab* 21:443-54.
- 1196 Lee SR, Kim HK, Song IS, Youm J, Dizon LA, Jeong SH, Ko TH, Heo HJ, Ko KS, Rhee BD, Kim N, Han J (2013)  
1197 Glucocorticoids and their receptors: insights into specific roles in mitochondria. *Prog Biophys Mol Biol*  
1198 112:44-54.

- 1199 Leek BT, Mudaliar SR, Henry R, Mathieu-Costello O, Richardson RS (2001) Effect of acute exercise on citrate  
1200 synthase activity in untrained and trained human skeletal muscle. *Am J Physiol Regul Integr Comp*  
1201 *Physiol* 280:R441-7.
- 1202 Lemasters JJ, Nieminen AL, Qian T, Trost LC, Elmore SP, Nishimura Y, Crowe RA, Cascio WE, Bradham CA,  
1203 Brenner DA, Herman B (1998) The mitochondrial permeability transition in cell death: a common  
1204 mechanism in necrosis, apoptosis and autophagy. *Biochim Biophys Acta* 1366:177-96.
- 1205 Lemieux H, Blier PU, Gnaiger E (2017) Remodeling pathway control of mitochondrial respiratory capacity  
1206 by temperature in mouse heart: electron flow through the Q-junction in permeabilized fibers. *Sci Rep*  
1207 7:2840.
- 1208 Lemieux H, Semsroth S, Antretter H, Höfer D, Gnaiger E (2011) Mitochondrial respiratory control and early  
1209 defects of oxidative phosphorylation in the failing human heart. *Int J Biochem Cell Biol* 43:1729-38.
- 1210 Lenaz G, Tioli G, Falasca AI, Genova ML (2017) Respiratory supercomplexes in mitochondria. In:  
1211 Mechanisms of primary energy transduction in biology. M Wikstrom (ed) Royal Society of Chemistry  
1212 Publishing, London, UK:296-337.
- 1213 Ling C, Rönn T (2019) Epigenetics in human obesity and type 2 diabetes. *Cell Metab* 29:1028-44.  
1214 <https://doi.org/10.1016/j.cmet.2019.03.009>.
- 1215 Liu S, Roellig DM, Guo Y, Li N, Frace MA, Tang K, Zhang L, Feng Y, Xiao L (2016) Evolution of mitosome  
1216 metabolism and invasion-related proteins in *Cryptosporidium*. *BMC Genomics* 17:1006.
- 1217 Lisowski P, Kannan P, Mlody B, Prigione A (2018) Mitochondria and the dynamic control of stem cell  
1218 homeostasis. *EMBO Rep* 19:e45432.
- 1219 Luo S, Valencia CA, Zhang J, Lee NC, Slone J, Gui B, Wang X, Li Z, Dell S, Brown J, Chen SM, Chien YH, Hwu WL,  
1220 Fan PC, Wong LJ, Atwal PS, Huang T (2018) Biparental inheritance of mitochondrial DNA in humans.  
1221 *Proc Natl Acad Sci U S A* doi: 10.1073/pnas.1810946115.
- 1222 Margulis L (1970) Origin of eukaryotic cells. New Haven: Yale University Press.
- 1223 McDonald AE, Vanlerberghe GC, Staples JF (2009) Alternative oxidase in animals: unique characteristics and  
1224 taxonomic distribution. *J Exp Biol* 212:2627-34.
- 1225 McKenzie M, Lazarou M, Thorburn DR, Ryan MT (2006) Mitochondrial respiratory chain supercomplexes  
1226 are destabilized in Barth Syndrome patients. *J Mol Biol* 361:462-9.
- 1227 Menshikova EV, Ritov VB, Fairfull L, Ferrell RE, Kelley DE, Goodpaster BH (2006) Effects of exercise on  
1228 mitochondrial content and function in aging human skeletal muscle. *J Gerontol A Biol Sci Med Sci* 61:534-  
1229 40.
- 1230 Menshikova EV, Ritov VB, Ferrell RE, Azuma K, Goodpaster BH, Kelley DE (2007) Characteristics of skeletal  
1231 muscle mitochondrial biogenesis induced by moderate-intensity exercise and weight loss in obesity. *J*  
1232 *Appl Physiol* (1985) 103:21-7.
- 1233 Menshikova EV, Ritov VB, Toledo FG, Ferrell RE, Goodpaster BH, Kelley DE (2005) Effects of weight loss and  
1234 physical activity on skeletal muscle mitochondrial function in obesity. *Am J Physiol Endocrinol Metab*  
1235 288:E818-25.
- 1236 Miller GA (1991) The science of words. Scientific American Library New York:276 pp.
- 1237 Mitchell P (1961) Coupling of phosphorylation to electron and hydrogen transfer by a chemi-osmotic type  
1238 of mechanism. *Nature* 191:144-8.
- 1239 Mitchell P (2011) Chemiosmotic coupling in oxidative and photosynthetic phosphorylation. *Biochim*  
1240 *Biophys Acta Bioenergetics* 1807:1507-38.
- 1241 MitoEAGLE Task Group (2020) Mitochondrial physiology. 1. Mitochondria and bioblasts. *Bioenerg Commun*  
1242 2020.#.
- 1243 MitoEAGLE Task Group (2020) Mitochondrial physiology. 3. Mitochondrial markers. *Bioenerg Commun*  
1244 2020.#.
- 1245 Mogensen M, Sahlin K, Fernström M, Glintborg D, Vind BF, Beck-Nielsen H, Højlund K (2007) Mitochondrial  
1246 respiration is decreased in skeletal muscle of patients with type 2 diabetes. *Diabetes* 56:1592-9.
- 1247 Mohr PJ, Phillips WD (2015) Dimensionless units in the SI. *Metrologia* 52:40-7.
- 1248 Moreno M, Giacco A, Di Munno C, Goglia F (2017) Direct and rapid effects of 3,5-diiodo-L-thyronine (T2).  
1249 *Mol Cell Endocrinol* 7207:30092-8.
- 1250 Morrow RM, Picard M, Derbeneva O, Leipzig J, McManus MJ, Gouspillou G, Barbat-Artigas S, Dos Santos C,  
1251 Hepple RT, Murdock DG, Wallace DC (2017) Mitochondrial energy deficiency leads to hyperproliferation  
1252 of skeletal muscle mitochondria and enhanced insulin sensitivity. *Proc Natl Acad Sci U S A* 114:2705-10.
- 1253 Murley A, Nunnari J (2016) The emerging network of mitochondria-organelle contacts. *Mol Cell* 61:648-53.
- 1254 National Academies of Sciences, Engineering, and Medicine (2018) International coordination for science  
1255 data infrastructure: Proceedings of a workshop—in brief. Washington, DC: The National Academies  
1256 Press. doi: <https://doi.org/10.17226/25015>.

- 1257 Oemer G, Lackner L, Muigg K, Krumschnabel G, Watschinger K, Sailer S, Lindner H, Gnaiger E, Wortmann SB,  
1258 Werner ER, Zschocke J, Keller MA (2018) The molecular structural diversity of mitochondrial  
1259 cardiolipins. *Proc Nat Acad Sci U S A* 115:4158-63.
- 1260 Palmfeldt J, Bross P (2017) Proteomics of human mitochondria. *Mitochondrion* 33:2-14.
- 1261 Paradies G, Paradies V, De Benedictis V, Ruggiero FM, Petrosillo G (2014) Functional role of cardiolipin in  
1262 mitochondrial bioenergetics. *Biochim Biophys Acta* 1837:408-17.
- 1263 Pesta D, Gnaiger E (2012) High-Resolution Respirometry. OXPHOS protocols for human cells and  
1264 permeabilized fibres from small biopsies of human muscle. *Methods Mol Biol* 810:25-58.
- 1265 Pesta D, Hoppel F, Macek C, Messner H, Faulhaber M, Kobel C, Parson W, Burtscher M, Schocke M, Gnaiger E  
1266 (2011) Similar qualitative and quantitative changes of mitochondrial respiration following strength and  
1267 endurance training in normoxia and hypoxia in sedentary humans. *Am J Physiol Regul Integr Comp*  
1268 *Physiol* 301:R1078-87.
- 1269 Price TM, Dai Q (2015) The role of a mitochondrial progesterone receptor (PR-M) in progesterone action.  
1270 *Semin Reprod Med* 33:185-94.
- 1271 Puchowicz MA, Varnes ME, Cohen BH, Friedman NR, Kerr DS, Hoppel CL (2004) Oxidative phosphorylation  
1272 analysis: assessing the integrated functional activity of human skeletal muscle mitochondria – case  
1273 studies. *Mitochondrion* 4:377-85. Puntschart A, Claassen H, Jostarndt K, Hoppeler H, Billeter R (1995)  
1274 mRNAs of enzymes involved in energy metabolism and mtDNA are increased in endurance-trained  
1275 athletes. *Am J Physiol* 269:C619-25.
- 1276 Quiros PM, Mottis A, Auwerx J (2016) Mitonuclear communication in homeostasis and stress. *Nat Rev Mol*  
1277 *Cell Biol* 17:213-26.
- 1278 Rackham O, Mercer TR, Filipovska A (2012) The human mitochondrial transcriptome and the RNA-binding  
1279 proteins that regulate its expression. *WIREs RNA* 3:675-95.
- 1280 Rackham O, Shearwood AM, Mercer TR, Davies SM, Mattick JS, Filipovska A (2011) Long noncoding RNAs  
1281 are generated from the mitochondrial genome and regulated by nuclear-encoded proteins. *RNA*  
1282 17:2085-93.
- 1283 Reichmann H, Hoppeler H, Mathieu-Costello O, von Bergen F, Pette D (1985) Biochemical and  
1284 ultrastructural changes of skeletal muscle mitochondria after chronic electrical stimulation in rabbits.  
1285 *Pflugers Arch* 404:1-9.
- 1286 Renner K, Amberger A, Konwalinka G, Gnaiger E (2003) Changes of mitochondrial respiration,  
1287 mitochondrial content and cell size after induction of apoptosis in leukemia cells. *Biochim Biophys Acta*  
1288 1642:115-23.
- 1289 Rice DW, Alverson AJ, Richardson AO, Young GJ, Sanchez-Puerta MV, Munzinger J, Barry K, Boore JL, Zhang  
1290 Y, dePamphilis CW, Knox EB, Palmer JD (2016) Horizontal transfer of entire genomes via mitochondrial  
1291 fusion in the angiosperm *Amborella*. *Science* 342:1468-73.
- 1292 Rich P (2003) Chemiosmotic coupling: The cost of living. *Nature* 421:583.
- 1293 Rich PR (2013) Chemiosmotic theory. *Encyclopedia Biol Chem* 1:467-72.
- 1294 Roger JA, Munoz-Gomes SA, Kamikawa R (2017) The origin and diversification of mitochondria. *Curr Biol*  
1295 27:R1177-92.
- 1296 Rostovtseva TK, Sheldon KL, Hassanzadeh E, Monge C, Saks V, Bezrukov SM, Sackett DL (2008) Tubulin  
1297 binding blocks mitochondrial voltage-dependent anion channel and regulates respiration. *Proc Natl*  
1298 *Acad Sci USA* 105:18746-51.
- 1299 Rustin P, Parfait B, Chretien D, Bourgeron T, Djouadi F, Bastin J, Rötig A, Munnich A (1996) Fluxes of  
1300 nicotinamide adenine dinucleotides through mitochondrial membranes in human cultured cells. *J Biol*  
1301 *Chem* 271:14785-90.
- 1302 Saks VA, Veksler VI, Kuznetsov AV, Kay L, Sikk P, Tiivel T, Tranqui L, Olivares J, Winkler K, Wiedemann F,  
1303 Kunz WS (1998) Permeabilised cell and skinned fiber techniques in studies of mitochondrial function in  
1304 vivo. *Mol Cell Biochem* 184:81-100.
- 1305 Salabei JK, Gibb AA, Hill BG (2014) Comprehensive measurement of respiratory activity in permeabilized  
1306 cells using extracellular flux analysis. *Nat Protoc* 9:421-38.
- 1307 Sazanov LA (2015) A giant molecular proton pump: structure and mechanism of respiratory complex I. *Nat*  
1308 *Rev Mol Cell Biol* 16:375-88.
- 1309 Schneider TD (2006) Claude Shannon: biologist. The founder of information theory used biology to  
1310 formulate the channel capacity. *IEEE Eng Med Biol Mag* 25:30-3.
- 1311 Schönfeld P, Dymkowska D, Wojtczak L (2009) Acyl-CoA-induced generation of reactive oxygen species in  
1312 mitochondrial preparations is due to the presence of peroxisomes. *Free Radic Biol Med* 47:503-9.
- 1313 Schultz J, Wiesner RJ (2000) Proliferation of mitochondria in chronically stimulated rabbit skeletal muscle-  
1314 -transcription of mitochondrial genes and copy number of mitochondrial DNA. *J Bioenerg Biomembr*  
1315 32:627-34.



- 1316 Simson P, Jepihhina N, Laasmaa M, Peterson P, Birkedal R, Vendelin M (2016) Restricted ADP movement in  
 1317 cardiomyocytes: Cytosolic diffusion obstacles are complemented with a small number of open  
 1318 mitochondrial voltage-dependent anion channels. *J Mol Cell Cardiol* 97:197-203.
- 1319 Singh BK, Sinha RA, Tripathi M, Mendoza A, Ohba K, Sy JAC, Xie SY, Zhou J, Ho JP, Chang CY, Wu Y, Giguère V,  
 1320 Bay BH, Vanacker JM, Ghosh S, Gauthier K, Hollenberg AN, McDonnell DP, Yen PM (2018) Thyroid  
 1321 hormone receptor and ERR $\alpha$  coordinately regulate mitochondrial fission, mitophagy, biogenesis, and  
 1322 function. *Sci Signal* 11(536) DOI: 10.1126/scisignal.aam5855.
- 1323 Speijer D (2016) Being right on Q: shaping eukaryotic evolution. *Biochem J* 473:4103-27.
- 1324 Stucki JW, Ineichen EA (1974) Energy dissipation by calcium recycling and the efficiency of calcium  
 1325 transport in rat-liver mitochondria. *Eur J Biochem* 48:365-75.
- 1326 Sugiura A, Mattie S, Prudent J, McBride HM (2017) Newly born peroxisomes are a hybrid of mitochondrial  
 1327 and ER-derived pre-peroxisomes. *Nature* 542:251-4.
- 1328 Tonkonogi M, Harris B, Sahlin K (1997) Increased activity of citrate synthase in human skeletal muscle after  
 1329 a single bout of prolonged exercise. *Acta Physiol Scand* 161:435-6.
- 1330 Torralba D, Baixauli F, Sánchez-Madrid F (2016) Mitochondria know no boundaries: mechanisms and  
 1331 functions of intercellular mitochondrial transfer. *Front Cell Dev Biol* 4:107. eCollection 2016.
- 1332 Vamecq J, Schepers L, Parmentier G, Mannaerts GP (1987) Inhibition of peroxisomal fatty acyl-CoA oxidase  
 1333 by antimycin A. *Biochem J* 248:603-7.
- 1334 Waczulikova I, Habodaszova D, Cagalinec M, Ferko M, Ulicna O, Mateasik A, Sikurova L, Ziegelhöffer A (2007)  
 1335 Mitochondrial membrane fluidity, potential, and calcium transients in the myocardium from acute  
 1336 diabetic rats. *Can J Physiol Pharmacol* 85:372-81.
- 1337 Wagner BA, Venkataraman S, Buettner GR (2011) The rate of oxygen utilization by cells. *Free Radic Biol*  
 1338 *Med* 51:700-712.
- 1339 Wang H, Hiatt WR, Barstow TJ, Brass EP (1999) Relationships between muscle mitochondrial DNA content,  
 1340 mitochondrial enzyme activity and oxidative capacity in man: alterations with disease. *Eur J Appl Physiol*  
 1341 *Occup Physiol* 80:22-7.
- 1342 Watt IN, Montgomery MG, Runswick MJ, Leslie AG, Walker JE (2010) Bioenergetic cost of making an  
 1343 adenosine triphosphate molecule in animal mitochondria. *Proc Natl Acad Sci U S A* 107:16823-7.
- 1344 Weibel ER, Hoppeler H (2005) Exercise-induced maximal metabolic rate scales with muscle aerobic  
 1345 capacity. *J Exp Biol* 208:1635-44.
- 1346 White DJ, Wolff JN, Pierson M, Gemmell NJ (2008) Revealing the hidden complexities of mtDNA inheritance.  
 1347 *Mol Ecol* 17:4925-42.
- 1348 Wikström M, Hummer G (2012) Stoichiometry of proton translocation by respiratory complex I and its  
 1349 mechanistic implications. *Proc Natl Acad Sci U S A* 109:4431-6.
- 1350 Williams EG, Wu Y, Jha P, Dubuis S, Blattmann P, Argmann CA, Houten SM, Amariuta T, Wolski W, Zamboni  
 1351 N, Aebbersold R, Auwerx J (2016) Systems proteomics of liver mitochondria function. *Science* 352  
 1352 (6291):aad0189
- 1353 Willis WT, Jackman MR, Messer JI, Kuzmiak-Glancy S, Glancy B (2016) A simple hydraulic analog model of  
 1354 oxidative phosphorylation. *Med Sci Sports Exerc* 48:990-1000.
- 1355 Yoshinaga MY, Kellermann MY, Valentine DL, Valentine RC (2016) Phospholipids and glycolipids mediate  
 1356 proton containment and circulation along the surface of energy-transducing membranes. *Prog Lipid Res*  
 1357 64:1-15.
- 1358 Zíková A, Hampl V, Paris Z, Týč J, Lukeš J (2016) Aerobic mitochondria of parasitic protists: diverse genomes  
 1359 and complex functions. *Mol Biochem Parasitol* 209:46-57.

1360  
 1361

1362 **\*Authors (MitoEAGLE Task Group): for list of authors and affiliations, see:**

1363 [https://www.bioenergetics-communications.org/index.php/BEC2020.1\\_doi10.26124bec2020-0001.v1](https://www.bioenergetics-communications.org/index.php/BEC2020.1_doi10.26124bec2020-0001.v1)

1364

1365 **Author contributions:** This manuscript developed as an open invitation to scientists and students to join  
 1366 as coauthors in the bottom-up spirit of COST, based on a first draft written by the corresponding author,  
 1367 who integrated coauthor contributions in a sequence of Open Access versions. Coauthors contributed to the  
 1368 scope and quality of the manuscript, may have focused on a particular section, and are listed in alphabetical  
 1369 order. Coauthors confirm that they have read the final manuscript and agree to implement the  
 1370 recommendations into future manuscripts, presentations and teaching materials.

1371

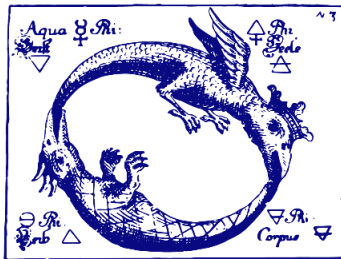


## COST Action CA15203 MitoEAGLE

1372 **Acknowledgements:** We thank Marija Beno for management assistance, and Peter R Rich for valuable  
 1373 discussions. This publication is based upon work from COST Action MitoEAGLE, supported by COST  
 1374 (European Cooperation in Science and Technology), in cooperation with COST Actions CA16225 EU-  
 1375 CARDIOPROTECTION and CA17129 CardioRNA; K-Regio project MitoFit funded by the Tyrolian  
 1376 Government, and project NextGen-O2k which has received funding from the European Union's Horizon  
 1377 2020 research and innovation programme under grant agreement No. 859770.

1378  
 1379 **Competing financial interests:** Erich Gnaiger is founder and CEO of Oroboros Instruments, Innsbruck,  
 1380 Austria.

1381  
 1382 **Corresponding author:** Erich Gnaiger  
 1383 Chair COST Action CA15203 MitoEAGLE – <http://www.mitoeagle.org>  
 1384 Department of Visceral, Transplant and Thoracic Surgery, D. Swarovski Research Laboratory, Medical  
 1385 University of Innsbruck, Innrain 66/4, A-6020 Innsbruck, Austria  
 1386 Email: [mitoeagle@i-med.ac.at](mailto:mitoeagle@i-med.ac.at); Tel: +43 512 566796, Fax: +43 512 566796 20  
 1387



BIOENERGETICS  
COMMUNICATIONS

1388 **Copyright:** © 2020 The authors. This is an Open Access communication distributed under the terms of the  
 1389 Creative Commons Attribution License, which permits unrestricted use, distribution, and reproduction in  
 1390 any medium, provided the original authors and source are credited. © remains with the authors, who have  
 1391 granted Bioenergetics Communications an Open Access publication licence in perpetuity.